

Markov-Switching State Space Models for Uncovering Musical Interpretation

Daniel J. McDonald^{a,1}, Michael McBride^b, Yupeng Gu^c, and Christopher Raphael^c

^aDepartment of Statistics, The University of British Columbia

^bDepartment of Statistics, Indiana University

^cSchool of Informatics, Computing, and Engineering, Indiana University

Last updated: 1 September 2021

Abstract

For concertgoers, musical interpretation is the most important factor in determining whether or not we enjoy a classical performance. Every performance includes mistakes—intonation issues, a lost note, an unpleasant sound—but these are all easily forgotten (or unnoticed) when a performer engages her audience, imbuing a piece with novel emotional content beyond the vague instructions inscribed on the printed page. In this research, we use data from the CHARM Mazurka Project—forty-six professional recordings of Chopin’s Mazurka Op. 68 No. 3 by consummate artists—with the goal of elucidating musically interpretable performance decisions. We focus specifically on each performer’s use musical tempo by examining the inter-onset intervals of the note attacks in the recording. To explain these tempo decisions, we develop a switching state space model and estimate it by maximum likelihood combined with prior information gained from music theory and performance practice. We use the estimated parameters to quantitatively describe individual performance decisions and compare recordings. These comparisons suggest methods for informing music instruction, discovering listening preferences, and analyzing performances.

Contents

1	Introduction	2
1.1	Related work	4
1.2	Our contributions	5

¹To whom correspondence should be addressed. E-mail: daniel@stat.ubc.ca. This work began while DJM was a member of the Department of Statistics at Indiana University. This work was partially supported by the National Science Foundation Grants DMS-1407439 and DMS-1753171 (to DJM) and Grant IIS-1526473 (to CR).

2	Materials and methods	6
2.1	Switching state-space models	6
2.2	A model for tempo decisions	7
2.3	Estimation and computational issues	12
2.4	Penalized maximum likelihood	13
2.5	Is this model reasonable	13
3	Analysis of Chopin’s Mazurka Op. 68 No. 3	15
3.1	Musical analysis	15
3.2	Archetypal performances	16
3.3	Comparing performances	18
3.4	Alternative smoothers	22
3.5	Problems with the model and estimation	24
3.6	Prior sensitivity and generalization	25
4	Discussion	25
A	Supplementary material	33
A.1	Algorithms	33
A.2	Principal components	33
A.3	Confidence intervals	35
A.4	Distance matrix from raw data	35
A.5	Plotting performances	37
A.6	Investigation of oversmoothing	37
A.7	Distribution over states	38
A.8	Multiplicative tempo changes	38
A.9	Alternative prior distributions	39

1 Introduction

Statistical analysis of the musical content of recordings has become more and more important to academics and industry. Online music services like Pandora, Last.fm, Spotify, and others rely on recommendation systems to suggest potentially interesting or related songs to listeners. In 2011, the KDD Cup challenged academic computer scientists and statisticians to identify user tastes in music with the [Yahoo! Million Song Dataset](#) (see [Dror et al. \(2012\)](#) for details of the competition). Pandora, through its proprietary [Music Genome Project](#), uses trained musicologists to assign new songs a vector of trait expressions (consisting of up to 500 “genes” depending on the genre) which can then be used to measure similarity with other songs. However, most of this work has focused on the analysis of more popular and more profitable genres of music—pop, rock, country—as opposed to classical music.

Western classical music is a subcategory whose boundaries are occasionally difficult to define. But the distinction is of great importance when it comes to the analysis which we undertake here. Leonard Bernstein, the great composer, conductor, and pianist, gave the following characterization in one of his famous “Young People’s Concerts” broadcast by the Columbia Broadcasting Corporation in the 1950s and 1960s ([Bernstein, 2005](#)).

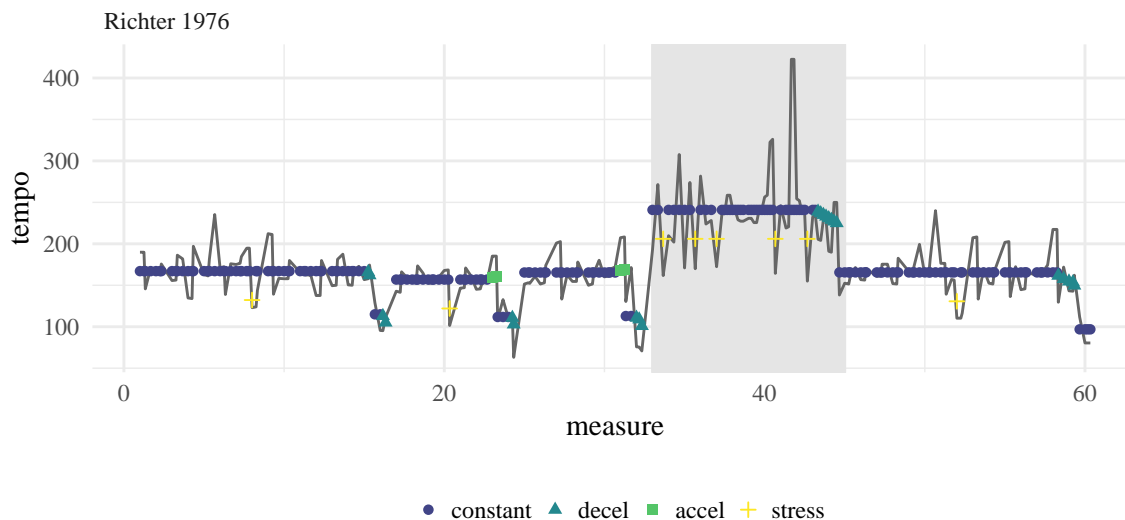


Figure 1: Note-by-note tempos for a recording of Chopin’s Mazurka Op. 68 No. 3 by Sviatoslav Richter. The solid line are the observed tempos, while the dots represent inferred tempo states from our model.

[. . . W]hen a composer writes a piece of what’s usually called classical music, he puts down the exact notes that he wants, the exact instruments or voices that he wants to play or sing those notes [. . .] and he also writes down as many directions as he can think of. [. . .] Of course, no performance can be perfectly exact, because there aren’t enough words in the world to tell the performers everything they have to know about what the composer wanted.

What separates classical music from other types of music is that the music itself is written down very precisely but performed millions of times in a variety of interpretations.¹ There is no “gold standard” recording to which everyone can refer but rather a document created for reference. Therefore, the musical genome technique mentioned above will only relate “pieces” but not “performances”. We need new methods to decide whether we prefer Leonard Bernstein’s recording of Beethoven’s Fifth Symphony or Herbert von Karajan’s and to articulate why.

In this paper, we develop a statistical model for some of the decisions that a musician must make for classical music interpretations. We focus on how the musician modulates *tempo*, or speed, over the course of a recording. Figure 1 shows the tempo² in beats-per-minute (b.p.m.) of a recording made by Sviatoslav Richter of Chopin’s Mazurka Op. 68 No. 3. The solid line shows the actual tempo at which he plays each note, while the points correspond to our model’s inferences for his actual intentions. Some of this intent is prescribed by Chopin in

¹Of course jazz, rock, pop and other genres are often written down for future performances, but without the same precision. Compare for example a lead sheet John Coltrane’s “Giant Steps” to his original 1960 recording.

²Technically, by “tempo”, we mean the ratio of musical time to clock time as 0.25 beats / 0.1 seconds = 150 beats per minute. A musician would likely think of “tempo” more broadly as something like a “typical speed regime” akin to the “constant tempo” state we use in our decision model below. We will not generally distinguish between these two interpretations and use the more succinct “tempo”.

his music, but the extent to which Richter observes Chopin’s indications makes his recording different from those of other pianists. It is these differences that we hope to capture and understand.

1.1 Related work

The vast majority of work at the intersection of statistics and classical music analysis has focused on a handful of tasks, most notably structure analysis, music generation, and score alignment.

Analysis of musical structure and its relationships with interpretation forms the basis of music theory, and hence constitutes the core of standard conservatory curricula, along with history and performance. Automatically discovering musical structures from performances without expert input has become more relevant recently. Ren et al. (2010) use Dirichlet process models to identify similar sections of individual classical music performances. Roberts et al. (2018a) use variational autoencoders to discover long-term structure with an explicit goal toward improved automatic music composition.

Computer music generation and composition has a long history (Sturm et al., 2019; Boulanger-Lewandowski et al., 2012; Collins, 2016; Ariza, 2005; Flossmann et al., 2013). It is actively investigated, especially using deep learning (Hadjeres et al., 2017), and has become commercially relevant for advertising and video games through companies like Aiva (aiva.ai), and Melodrive (melodrive.com). Google has developed the Magenta project to enable open-source music composition (Roberts et al., 2018b).

The score alignment problem matches live or recorded performances to the musical score, a necessary processing step for any automated analysis. On-line alignment processes audio waveforms in real-time and is sometimes called score following (Dannenberg and Raphael, 2006; Cont, 2010; Cont et al., 2007; Arzt and Widmer, 2015). Audio matched to the score can then be used as an input for automated musical accompaniment (Raphael, 2010; Vercoe, 1984; Dannenberg, 1985). Given recorded accompaniment, these systems modulate playback in response to a live soloist who both makes interpretive timing decisions and mistakes. Off-line alignment (Earis, 2007) can be used to analyze the recordings, as we do here, or for generating descriptive features of the performance (Thickstun et al., 2017), possibly for later analysis in recommender systems (McFee and Lanckriet, 2011; van den Oord et al., 2013). For an overview of related goals in music information retrieval, see Schedl et al. (2014).

More closely connected to the work here is the literature on expressive synthesis (Grindlay and Helmbold, 2006; Flossman S. Grachten and Widmer, 2012; Widmer et al., 2009; Maezawa, 2019; Bresin et al., 2002; Arcos and Mantaras, 2001). In this domain, one seeks to create a musically satisfying performance of a score, often given a training set of score-performance pairs. This problem is highly challenging since musical interpretation relies on latent aspects of the music, such as structure, stress, grouping, closure, surprise, affect, and others not explicitly appearing in the score. Music theorists often describe the score as the *surface* of the music, thus recognizing that there is much that lies beneath this surface. Though we do not treat expressive synthesis, our work shares the need for explicitly representing expressive performances.

Most recent work in expressive synthesis is based in machine learning, both in terms of methodology and the agnostic spirit of the modeling. Here one parametrizes the performance

in terms of variables that will be estimated from the score, such as rate of change of tempo or dynamics. For instance, [Flossman S. Grachten and Widmer \(2012\)](#) represent the joint configuration of local performance parameters and score parameters as a conditional Gaussian distribution, learned from training, and then used to estimate the expression on a new score. We also use conditional Gaussians as a modeling element, though we try to model the *process* nature of the music, rather than viewing each note independently. The work on expressive synthesis of [Maezawa \(2019\)](#) uses an autoregression to model the expressive parameters of a note, estimating the autoregressive parameters using deep learning on score attributes. The use of autoregression accomodates the smoothness normally found in expressive performance, while still not being overly prescriptive about the nature of the musical evolution.

Common to these approaches are the generic assumptions relating the musical score and the expressive performance parameters, hoping to push the hardest work — understanding what is important — onto the learning algorithm. In this spirit one seeks to discover what relevant sub-surface attributes of the score can be correlated with performance decisions. Perhaps the most extreme example of this musically agnostic approach is [Grindlay and Helmbold \(2006\)](#), who use a minimally-primed hidden Markov model to generate expression without giving any explicit meaning to the states.

We emphasize an important modeling difference between these approaches and what we propose. We explicitly model the performance in terms of a switching Kalman filter, thus making rather strong *a priori* assumptions derived from our musical sensibilities. [Stowell and Chew \(2012\)](#) similarly use an explicit parametrization of tempo evolution by automatically partitioning the music into segments represented by local quadratics. Our approach considers a broader family of parametrizations but shares the basic approach of *building in* musical knowledge to the model.

1.2 Our contributions

In this paper, we develop a switching Kalman filter model for the tempo decisions a performer makes in recorded classical music. We present an algorithm for performing likelihood inference, estimate our model using a large collection of recordings of the same composition, and demonstrate how the model is able to recover performer intentions, and how they relate to standard musical analysis. We use the low-dimensional representations to compare and contrast the recordings, and discuss how this analysis facilitates more informed musical comparisons of the recordings. Such an analysis may help listeners to choose other performers whose tendencies are similar (or dramatically different!) from those they already enjoy, suggest new recordings to purchase, or motivate future concert attendance behaviors. Our analysis can also aid automatic performance generation by reusing a musician’s estimated parameters on a reproducing instrument or potentially inform music education. In combination with other software, a music teacher could create visuals for a student’s performance, such as those presented in this paper, and directly discuss areas for improvement.

In [Section 2](#) we discuss our dataset, a collection of professional recordings of Chopin’s Mazurka Op. 68 No. 3. We also present our model for tempo decisions, discuss its statistical estimation, and detail its utility for understanding interpretations as a musician would. [Section 3](#) presents a music theory interpretation of the Mazurka. We discuss how different performers approach this piece through the lens of our model. We also examine groups of

performances based on our model and interpret the musical meaning of these groupings. Finally, we contrast our approach with some alternative non-parametric smoothers, discuss their deficiencies relative our switching model, and examine some issues with our proposal.

2 Materials and methods

In this paper, we examine note-by-note tempos for 46 recordings of Chopin’s Mazurka Op. 68, No. 3. The data is part of a large collection of the complete Chopin Mazurkas and other recordings assembled and analyzed by the Center for the History and Analysis of Recorded Music (CHARM) in the United Kingdom (CHARM, 2009). The recordings were processed using the note-onset detection algorithm developed by Earis (2007) and are available for download (Earis, 2009). We use the data for “all rhythmic events”, which includes the time of each note attack as well as its relative loudness.

2.1 Switching state-space models

State-space models define the probability distribution of a continuous time series Y by reference to some imagined, continuous hidden state, X . In particular, the observation at time i is assumed to be independent of past and future observations conditional on the state at time i . Coupling with temporal dependence for X —most frequently obeying the Markov property—induces a temporal model for the observations. The most general form of a state-space model is then characterized by the measurement equation (the conditional probability of observations given the states), the transition equation (specifying the nature of Markovian dynamics), and an initial distribution for the state:

$$y_i = f_\theta(x_i, \epsilon_i), \quad x_{i+1} = g_\theta(x_i, \eta_i), \quad x_1 \sim F, \quad (1)$$

where ϵ_i are η_i are marginally and mutually independent and F is an arbitrary but specified distribution. Both y_i and x_i can be vector-valued, though in our application, y_i will be univariate. The vector $\{y_i\}_{i=1}^n$ is observed, and the goal is to make inferences for the unobserved states $\{x_i\}_{i=1}^n$ as well as any unknown parameters θ characterizing f_θ , g_θ , and the distributions of ϵ_i and η_i .

If f_θ and g_θ are linear, and ϵ_i , η_i , and F assumed to have Gaussian distributions, Equation (1) becomes

$$\begin{aligned} x_{i+1} &= d + Tx_i + \eta_i, & \eta_i &\sim N(0, Q), & x_1 &\sim N(x_0, P_0), \\ y_i &= c + Zx_i + \epsilon_i, & \epsilon_i &\sim N(0, G), \end{aligned} \quad (2)$$

where the vectors c , d and matrices T , Z , Q , and G are allowed to depend on θ , can potentially vary with i , or can depend on previous values of x and y . In this case, the Kalman filter (see for example, Kalman, 1960; Harvey, 1990), provides closed form solutions for the conditional distributions of the states and gives the likelihood of θ given data. For completeness, we have included the Kalman filter inference algorithm in the Supplement (McDonald et al., 2021).

Although the Kalman filter returns the likelihood for θ , and is therefore all we need for parameter estimation, inference for the mean and variance of X is conditional only on

the preceding observations $\{y_j\}_{j=1}^i$: $X_i = E[x_i | y_1, \dots, y_i]$ and $P_i = Var[x_i | y_1, \dots, y_i]$. To incorporate all future observations into these estimates, and produce the inferred performance tempos shown in, for example, [Figure 1](#), the Kalman smoother is required. Many different smoother algorithms have been tailored for different applications. The smoother we use, due to [Rauch et al. \(1965\)](#), is often referred to as the classical fixed-interval smoother ([Anderson and Moore, 1979](#)). It produces only the unconditional expectations of the hidden state $\hat{x}_i = E[x_i | y_1, \dots, y_n]$, which is all that is necessary for our analysis. This algorithm is again given in the Supplementary Material ([McDonald et al., 2021](#)). We note that the smoother estimate of $Var[x_i | y_1, \dots, y_n]$ is not necessary for any of the analysis discussed in this paper.

Linear Gaussian state-space models can be made quite flexible by expanding the state vector or allowing the parameter matrices to vary with time. Furthermore, this general form encompasses many standard time series models: ARIMA models, ARCH and GARCH models, stochastic volatility models, exponential smoothers, and more (see [Durbin and Koopman, 2001](#), for many other examples). Nonlinear, non-Gaussian versions have been extensively studied ([Durbin and Koopman, 1997](#); [Fuh, 2006](#); [Kitagawa, 1987, 1996](#)) and algorithms for filtering, smoothing, and parameter estimation have been derived (for example, [Koyama et al., 2010](#); [Andrieu et al., 2010](#)). However, these models are less useful for change-point detection or other discontinuous behavior when the times of discontinuity are unknown.

To remedy this deficiency, one can use a switching state-space model as shown in [Figure 2](#). Here, we assume $\{s_i\}_{i=1}^n$ is a hidden, discrete process with Markovian dynamics. Then, the value of the hidden state at time i , $s_i = k$ say, can determine the evolution of the continuous model at time i . The graphical model in [Figure 2](#) gives the conditional independence properties we will use in our model for musical interpretation, representing just one of many possibilities. Switching state-space models have a long history with applications ranging from economics ([Kim and Nelson, 1998](#); [Kim, 1994](#); [Hamilton, 2011](#)) to speech processing ([Fox et al., 2011](#)) to animal movement ([Patterson et al., 2008](#); [Block et al., 2011](#)). [Ghahramani and Hinton \(2000\)](#) provide an excellent overview of the history, typography, and algorithmic developments. In Equation (2), the parameter matrices were not time varying. We allow the switch states s_i, s_{i-1} , along with the parameter vector θ , to determine the specific dynamics at time i :

$$\begin{aligned} x_1 &\sim N(x_0, P_0), \\ x_{i+1} &= d(s_i, s_{i-1}) + T(s_i, s_{i-1})x_i + \eta_i, \quad \eta_i \sim N(0, Q(s_i, s_{i-1})), \\ y_i &= c(s_i) + Z(s_i)x_i + \epsilon_i, \quad \epsilon_i \sim N(0, G(s_i)). \end{aligned}$$

In other words, the hidden Markov (switch) state determines the collection of d , c , T , Z , G and Q that govern the evolution of the system. Allowing d , T , and Q , to depend on s_{i-1} in addition to s_i (the diagonal arrow in [Figure 2](#)) will allow us to incorporate acceleration as well as velocity into our model for tempo decisions.

2.2 A model for tempo decisions

In musical scores, *tempi* (the Italian plural of tempo) may be marked at various points throughout a piece of music. The beginning can be either explicit, with a metronome marking to indicate the number of beats per minute (b.p.m.), and/or with some words (e.g., *Adagio*, *Presto*, *Langsam*, Sprightly) which indicate an approximate speed. [Figure 3](#) shows

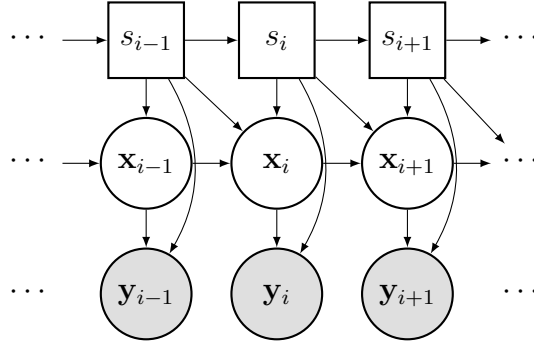


Figure 2: Switching state space model. Filled objects are observed, rectangles are discrete, and circles are continuous.



Figure 3: The beginning of two Chopin piano compositions: the Mazurka we analyze is on the left while the Ballade No. 1, Op. 23 is on the right.

the beginning of two Chopin piano compositions: the Mazurka we analyze and the Ballade No. 1, Op. 23. The initial tempo of the Mazurka is given with a metronome marking as well as the Italian phrase *Allegro ma non troppo* (“cheerful, but not too much”). The beginning of the Ballade is marked *Largo*, which translates literally as “broad” or “wide”, and modified by the stylistic indication *pesante* (“heavy”). Obviously, the metronome markings are much more exact, though even these are often viewed as suggestions rather than commandments. The metronome markings in most of Beethoven’s compositions, for example, are notoriously fast, and some scholars believe that his metronome (one of the first ever made) was inaccurate (Forsén et al., 2013). Often, compositions will have numerous such markings later in the piece of music, but these are only some of the ways that tempo is indicated. Composers will also indicate periods of speeding-up (*accelerando*) or slowing-down (*ritardando*).

Absent instructions from the composer, performers generally maintain (or try to maintain) a steady tempo, and this assumption plays a major role in our model of tempo decisions. Of course, a normal human never plays precisely like a metronome, although she may try quite hard to do so. The observed ratio of musical time to clock time can therefore be thought of as stochastic, the sum of an intentional, constant tempo, plus noise representing inaccuracy or, perhaps more charitably, unintentional variation which the listener fails to perceive as “wrong”.³ For instance, the example in Figure 4 shows the beginning of the

³Some may argue with this explanation. As one anonymous reviewer pointed out, describing deviations from constant tempo as “unintentional noise” fails to account for the possibility that the performer is consciously or unconsciously controlling these small deviations, and their success as artists can be partially attributed to their preternatural abilities to exert such control. In the end, our model is smoothing such deviations away for the sake of providing a low-dimensional explanation of performance behavior. See Section 2.5 for a discussion of how much might be lost by this smoothing.

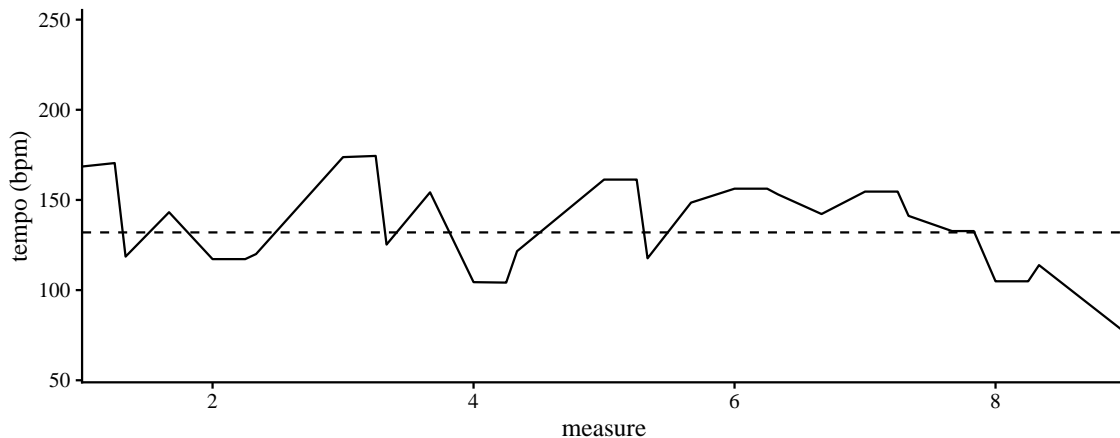


Figure 4: The solid line shows the observed note-by-note tempo for the beginning of the Mazurka as performed by Arthur Rubinstein in 1961. The dashed line indicates 132 b.p.m.

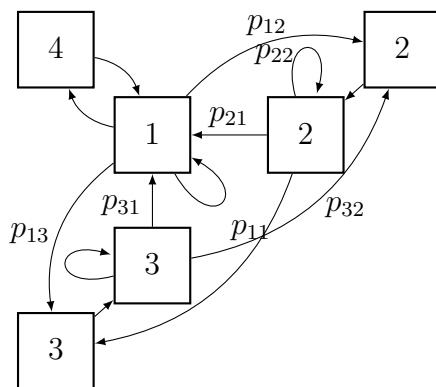


Figure 5: Transition diagram. The four states are: constant tempo (1), deceleration (2), acceleration (3), and emphasis (4).

piece as performed by Arthur Rubinstein in a 1961 recording. The solid line shows the actual, performed tempo, while the dashed horizontal line is placed at the indicated tempo of 132 b.p.m. The figure has three important lessons: (1) observed speed varies around intended tempo; (2) 132 b.p.m. is not necessarily the tempo a performer will choose despite the indication; and (3) performers have other tempo intentions which are not marked, like the pronounced slow-down in measures 7–8.

Estimating intended *tempi* would be reasonably simple, perhaps, if the locations of the tempo changes were known. In such a case, the average of tempi between changes may be a good estimate as could the slope of known speed-ups or slow-downs. However, performers take liberties with these decisions, exactly the liberties we would like to discover. This suggests employing a switching model with a small number of discrete states.

We propose a Markov model for S on four states for four different performance behaviors with transition probability diagram given by Figure 5. The 4 switch states correspond to 4 different behaviors for the performer: (1) constant tempo, (2) speeding up, (3) slowing down, and (4) single note stress. As shown in the diagram, we allow only certain transitions

for musical reasons and for estimability. The marked transition probabilities are sufficient to infer the remainder. One can imagine that a performer will remain mainly in the state 1 with departures to states 2 and 3 either due to markings by the composer, or, absent these, for interpretive reasons referred to collectively as *rubato*, which translates literally as “stolen time”. The fourth state, stress, corresponds to *tenuto*, a common feature of musical performance. These stresses may be marked with a line over the note in question, but are more often a feature of performer taste, corresponding to a longer-than-written duration for a particular note. Such emphases occur for a variety of musical purposes—emphasis of the beat in running notes, the top of a phrase, a “landing point” where a phrase ends, etc.—but are always within the frame of constant tempo. Thus we allow stress to occur only after and before notes in state 1. Furthermore, we cannot allow state 2 or state 3 to return immediately to state 1, or else “stress” could happen through these pathways. We impose related constraints for a transition from state 2 to state 3 and vice versa. Essentially, transitions into these states must remain there before leaving. Thus, the entire transition diagram is fully determined. This process can be viewed equivalently as a second-order Markov chain.

Generally, we feel that this model should be broadly applicable across composers and time periods as well as instrumentation. That is, it should work equally well for compositions by Mozart, Bach, Beethoven, or Stravinsky. While some composers, especially those that are more modern, have a more varied use of time signature and rhythm than the music we examine here, these generally require even more stringent adherence to “steady tempo”. Some of Chopin’s other compositions present more severe departures from steady tempo (the Nocturnes, for example), but we intend our model to be able to capture these features through states 3 or 4. We return to this issue in [Section 3.6](#).

Our data gives y_i as the observed tempo (in b.p.m.) of the note (or chord) of the i^{th} note onset in Chopin’s Mazurka Op. 68 No. 3. The hidden continuous variable (X_i) is taken to be a two component vector with the first component being the prevailing tempo and the second the amount of acceleration. The amount, or existence, of acceleration is determined by the current and previous switch states. We use ℓ_i to denote the musical duration of a particular note as given by the written score. Because, in this piece, each measure contains three quarter-notes, (♩), a quarter-note has $\ell_i = 1/3$, an eighth note (♪) has $\ell_i = 1/6$, etc. In more complicated music with changing time signatures or instances where the notation doesn’t necessarily correspond with the time signature, more care would be required. The observed tempo is already normalized to account for variable note durations, but the intentional tempo and its variance should be proportional to ℓ_i . When the performer is in state 1 (or transits in and out of state 4), we take the prevailing tempo as constant with no acceleration: $X_{i+1} = X_i$. Corresponding to these configurations, the parameter matrices are given in [Table 1](#) (transition equation) and [Table 2](#) (measurement equation). So for any performance, we wish to estimate the following parameters: σ_{tempo}^2 , σ_{acc}^2 , σ_{stress}^2 , σ_ϵ^2 , the probabilities of the transition matrix (there are 7), and means μ_{tempo} , μ_{acc} , and μ_{stress} . Lastly, we have the initial state distribution

$$x_1 \sim N \left(\begin{pmatrix} \mu_1 \\ 0 \end{pmatrix}, \begin{pmatrix} \sigma_1^2 & 0 \\ 0 & 0 \end{pmatrix} \right) \text{ where } s_1 = 1.$$

To clarify this model, we explicate two different behaviors: discrete sequence $1 \rightarrow 4 \rightarrow 1$

Table 1: Parameter matrices of the transition equation for the switching state space model.

Switch states		parameter matrices		
s_i	s_{i-1}	d	T	Q
1	1	0	$\begin{pmatrix} 1 & 0 \\ 0 & 0 \end{pmatrix}$	$\begin{pmatrix} 0 & 0 \\ 0 & 0 \end{pmatrix}$
2	1	$\begin{pmatrix} \ell_i \mu_{\text{acc}} \\ \mu_{\text{acc}} \end{pmatrix}$	$\begin{pmatrix} 1 & 0 \\ 0 & 0 \end{pmatrix}$	$\sigma_{\text{acc}}^2 \begin{pmatrix} \ell_i^2 & \ell_i \\ \ell_i & 1 \end{pmatrix}$
3	1	$\begin{pmatrix} -\ell_i \mu_{\text{acc}} \\ -\mu_{\text{acc}} \end{pmatrix}$	$\begin{pmatrix} 1 & 0 \\ 0 & 0 \end{pmatrix}$	$\sigma_{\text{acc}}^2 \begin{pmatrix} \ell_i^2 & \ell_i \\ \ell_i & 1 \end{pmatrix}$
4	1	$\begin{pmatrix} 0 \\ \mu_{\text{stress}} \end{pmatrix}$	$\begin{pmatrix} 1 & 0 \\ 0 & 0 \end{pmatrix}$	$\begin{pmatrix} 0 & 0 \\ 0 & \sigma_{\text{stress}}^2 \end{pmatrix}$
2	2	0	$\begin{pmatrix} 1 & \ell_i \\ 0 & 1 \end{pmatrix}$	$\begin{pmatrix} 0 & 0 \\ 0 & 0 \end{pmatrix}$
3	2	$\begin{pmatrix} -\ell_i \mu_{\text{acc}} \\ -\mu_{\text{acc}} \end{pmatrix}$	$\begin{pmatrix} 1 & 0 \\ 0 & 0 \end{pmatrix}$	$\sigma_{\text{acc}}^2 \begin{pmatrix} \ell_i^2 & \ell_i \\ \ell_i & 1 \end{pmatrix}$
1	2	$\begin{pmatrix} \mu_{\text{tempo}} \\ 0 \end{pmatrix}$	0	$\begin{pmatrix} \sigma_{\text{tempo}}^2 & 0 \\ 0 & 0 \end{pmatrix}$
3	3	0	$\begin{pmatrix} 1 & \ell_i \\ 0 & 1 \end{pmatrix}$	$\begin{pmatrix} 0 & 0 \\ 0 & 0 \end{pmatrix}$
2	3	$\begin{pmatrix} \ell_i \mu_{\text{acc}} \\ \mu_{\text{acc}} \end{pmatrix}$	$\begin{pmatrix} 1 & 0 \\ 0 & 0 \end{pmatrix}$	$\sigma_{\text{acc}}^2 \begin{pmatrix} \ell_i^2 & \ell_i \\ \ell_i & 1 \end{pmatrix}$
1	3	$\begin{pmatrix} \mu_{\text{tempo}} \\ 0 \end{pmatrix}$	0	$\begin{pmatrix} \sigma_{\text{tempo}}^2 & 0 \\ 0 & 0 \end{pmatrix}$
1	4	0	$\begin{pmatrix} 1 & 0 \\ 0 & 0 \end{pmatrix}$	$\begin{pmatrix} 0 & 0 \\ 0 & 0 \end{pmatrix}$

Table 2: Parameter matrices of the measurement equation for the switching state space model.

Switch states	parameter matrices		
s_i	c	Z	G
4	0	$\begin{pmatrix} 1 & 1 \end{pmatrix}$	σ_{ϵ}^2
else	0	$\begin{pmatrix} 1 & 0 \end{pmatrix}$	σ_{ϵ}^2

(emphasis within constant tempo) and discrete sequence $1 \rightarrow 1 \rightarrow 2$ (constant tempo to slowing down). In the first case, the state space system has the following configurations

$$\begin{array}{ll}
 1 \rightarrow 4 & 4 \rightarrow 1 \\
 x_2 = \begin{pmatrix} 0 \\ \mu_{\text{stress}} \end{pmatrix} + \begin{pmatrix} 1 & 0 \\ 0 & 0 \end{pmatrix} x_1 + \text{N} \left(0, \begin{pmatrix} 0 & 0 \\ 0 & \sigma_{\text{stress}}^2 \end{pmatrix} \right) & x_3 = \begin{pmatrix} 1 & 0 \\ 0 & 0 \end{pmatrix} x_2 \\
 y_2 = (1 \quad 1)x_2 + \text{N}(0, \sigma_\epsilon^2) & y_3 = (1 \quad 0)x_3 + \text{N}(0, \sigma_\epsilon^2),
 \end{array}$$

while in the second

$$\begin{array}{ll}
 1 \rightarrow 1 & 1 \rightarrow 2 \\
 x_2 = \begin{pmatrix} 1 & 0 \\ 0 & 0 \end{pmatrix} x_1 & x_3 = \begin{pmatrix} \ell_i \mu_{\text{acc}} \\ \mu_{\text{acc}} \end{pmatrix} + \begin{pmatrix} 1 & 0 \\ 0 & 0 \end{pmatrix} x_1 + \text{N} \left(0, \sigma_{\text{acc}}^2 \begin{pmatrix} \ell_i^2 & \ell_i \\ \ell_i & 1 \end{pmatrix} \right) \\
 y_2 = (1 \quad 0)x_2 + \text{N}(0, \sigma_\epsilon^2) & y_3 = (1 \quad 0)x_3 + \text{N}(0, \sigma_\epsilon^2).
 \end{array}$$

Recall that in any case y_i is a scalar and $x_i \in \mathbb{R}^2$.

2.3 Estimation and computational issues

To understand the performance decisions of individual musicians, we wish to simultaneously estimate θ , S , and X . Because the switch states S and the continuous states X are both hidden, this becomes an NP-hard problem. In particular, there are approximately 4^n possible paths through the switch variables, so evaluating the likelihood to maximize over θ via the Kalman filter at each path is intractable. Ghahramani and Hinton (2000) give a variational approximation to estimate θ without also estimating S , but, as our goal is to learn both, we use the particle filtering approximation described by Fearnhead and Clifford (2003). Whiteley et al. (2010) refer to this algorithm as the Discrete Particle Filter, and it can be seen as an instance of the ‘‘Beam Search’’ optimization technique (Bisiani, 1992). The details are given in Algorithm 1 but the intuition is as follows: (1) for the first few time points, evaluate one step of the Kalman filter for each possible subsequent discrete state and store all these values; (2) calculate weights for each path by updating previous weights with the likelihood multiplied by the transition probability; (3) continue through time until the number of stored values exceeds some threshold storage limit; (4) from that point forward, subselect the ‘‘best’’ paths using a sampling scheme. These paths can be selected greedily, retaining only the highest values to that point, though we use the resampling procedure of Fearnhead and Clifford (2003) which is designed to approximate the full discrete distribution over paths with a subset of support points by minimizing the mean squared error.

Algorithm 1 returns B paths through the discrete states along with their weights for a particular parameter value θ . One can view this as a (approximate) distribution over paths conditional on θ . Instead, we will simply take the path with the highest weight for inference via penalized maximum likelihood. Thus, the likelihood of a particular parameter vector θ is evaluated by computing the best path with Algorithm 1 and then using that best path with the Kalman filter.

Algorithm 1 Discrete particle filter

- 1: **Input:** Y, θ, π_1 probability vector over initial states (paths), B beam width
 - 2: **for** $i = 1$ **to** n **do**
 - 3: Set $b_i = |\{\pi_i > 0\}|$, the number of current paths
 - 4: Use the Kalman filter to calculate the 1-step likelihood \mathcal{L}_i for each path and every potential state s_{i+1} resulting in $b_i|S|$ particles
 - 5: Set $\pi_{i+1} \leftarrow \pi_i \mathcal{L}_i p_i$: multiply the path probability by the likelihood and the probability of transitioning. Normalize π .
 - 6: Set $b_{i+1} = |\{\pi_{i+1} > 0\}|$. If $b_{i+1} > B$, resample the weights to get B non-zero weights and renormalize
 - 7: **end for**
 - 8: Return B paths $\{S_b\}_{b=1}^B$ along with their weights π_n .
-

2.4 Penalized maximum likelihood

Even without the latent discrete process, parameter estimation in state-space models is a difficult problem, often plagued by spurious local minima and non-identifiability. The addition of discrete states only exacerbates this issue. However, for the present application, we have reasonable informative prior information for many of the parameters. The three mean parameters μ_{tempo} , μ_{acc} and μ_{stress} have sign restrictions in addition to reasonable constraints their magnitude: average tempo should be around the indicated 132 b.p.m., the average amount of acceleration should probably be less than the size of a stress. We also have can make musically informed choices about the probabilities of transitioning between states: self-transitions should be reasonably likely, long periods of speeding up are less likely than long periods of slowing down which are less likely than long periods in the constant tempo state.

Because of this information, we use informative priors as penalties on all the parameters we estimate. This has the effect of introducing extra curvature to the optimization problem as well as conforming with musical intuition. The specific choices are shown in Table 3. We fix σ_{acc}^2 and σ_{stress}^2 to be 1 after numerical experiments suggested that they were poorly identified. Essentially, large values of these variances make the stress and deceleration states difficult to separate, so other values of similar magnitude make little difference. Given the use of priors, one could interpret our procedure from a Bayesian perspective. However, we do not estimate full posteriors, only the maximum *a posteriori* value, so our prior specification choices are not intended to reflect tail uncertainty. We defer justification and discussion of these choices to Section 3.6.

2.5 Is this model reasonable

It is reasonable to ask whether a simple model such as this can accurately represent performance practice without removing musically important information. In a statistical sense, this question is similar to the problem of tuning parameter selection in nonparametric estimation. Specifically, we do not want this model to “over-smooth” the performance, eliminating information necessary for listener appreciation. One way to examine such a question is to generate a performance using the smoothed tempos resulting from the fitted model and compare it aurally with the original recording. Gu and Raphael (2012) evaluate this question empiri-

Table 3: Informative prior distributions for the music model

Parameter	Distribution	Prior mean
σ_ϵ^2	\sim Gamma(40, 10)	400 b.p.m. ²
μ_{tempo}	\sim Gamma($\bar{Y}^2/100$, $100/\bar{Y}$)	\bar{Y} b.p.m.
$-\mu_{\text{acc}}$	\sim Gamma(15, 2/3)	10 b.p.m.
$-\mu_{\text{stress}}$	\sim Gamma(20, 2)	40 b.p.m.
σ_{tempo}^2	\sim Gamma(40, 10)	400 b.p.m. ²
σ_{acc}^2	$=$ 1	1 b.p.m. ²
σ_{stress}^2	$=$ 1	1 b.p.m. ²
$p_{1,\cdot}$	\sim Dirichlet(85, 5, 2, 8)	
$p_{2,\cdot}$	\sim Dirichlet(4, 10, 1, 0)	
$p_{3,\cdot}$	\sim Dirichlet(5, 3, 7, 0)	

cally: they surveyed nine graduate piano majors at a major conservatory on twelve different piano excerpts, both performed and synthesized. The pianists were not meaningfully able to distinguish between the two in the majority of experiments. We expect that a similar study with our model would yield better results. In the Supplementary Material (McDonald et al., 2021), we allow the reader to decide for themselves: we have included a MIDI recording derived from Sviatoslav Richter’s 1976 recording as well as one synthesized using our model. The only difference is the tempos of the individual beats.

The generative model in Gu and Raphael (2012) is also a switching model on four states like ours. It is quite a bit simpler, however, in terms of the transition matrix depicted in Figure 5. It is only first-order, so states 2 and 3 can be entered and left immediately. There’s also no ability to go from state 3 to 2 or 2 to 1. This precludes the common feature of slowing down at the end of a phrase before returning to a new tempo. Furthermore, and importantly, their parameters are not estimated from data but chosen by eye. Comparing our model to theirs, we found that ours is more robust in that it is less likely to make spurious excursions to states 2 and 3 and more accurately uses state 4. It also has significantly lower RMSE on the data despite having only two additional parameters. A more careful comparison with this model is given in the Supplementary Material (McDonald et al., 2021).

While an additive state space model is relatively easy to understand, some music theorists (Mead, 2007, for example) have argued that musicians make multiplicative tempo adjustments. That is, the ratio between the tempo of the current note and that of the previous note is important rather than their difference. Such a conception is fundamental to musical notation (quarter notes, eighth notes, etc) and frequently used to specify tempo changes within a piece of music. Unfortunately, switching linear models are challenging to estimate and non-linear models are only more so. We examine a multiplicative model in the Supplementary Material. This model produces very reasonable interpretations of individual performances, but unfortunately, it is less useful for comparing performances.

3 Analysis of Chopin’s Mazurka Op. 68 No. 3

We use the model and procedures developed above to estimate the parameters and performance choices for all 46 recordings of Chopin’s Mazurka. Here we describe the inferences our model allows on some representative performances, describe performance groupings based on the estimated parameters, contrast our model with some alternative approaches to smoothing, and discuss some difficulties we encountered. All simulations and empirical calculations were performed with R (R Core Team, 2019) and C++ via Rcpp (Eddelbuettel, 2013). Figures and tables are generated using the `tidyverse` family of packages (Wickham, 2017, 2016). Most computations were implemented in parallel on a large memory computer cluster via the `batchtools` package (Lang et al., 2017).

3.1 Musical analysis

Throughout his life, Frédéric Chopin composed dozens of Mazurkas, of which 58 have been published. Inspired by a traditional Polish dance, these pieces gave Chopin an idiomatic style upon which to elaborate a wide variety of different compositional techniques, a practice German and Italian composers had employed frequently over the previous 3 centuries (Burkholder et al., 2014). Repetition of themes, figures, or even small motives plays a central role in both the traditional dance and Chopin’s compositions as do particular rhythmic gestures (Kallberg, 1996), especially the dotted-eighth sixteenth note pattern on the first beat of a measure.

Chopin’s Op. 68 Mazurkas are a set of four similar works, published posthumously in 1855. The Op. 68 No. 3, which we analyze here, was composed in 1830, when Chopin was 20 years old. Around this time, Chopin, already a piano virtuoso and accomplished composer, left his native Warsaw and settled in Paris, where we would remain until his death in 1849.

This Mazurka has a rather simplistic ternary structure with two outer sections and a contrasting middle (ABA). The first A section is made up of four eight-bar phrases (*aaba*). The first phrase is echoed by the second phrase: they are nearly identical, with the two exceptions being that (1) the second is marked *piano* (soft) rather *forte* (strong) and (2) the second ends on the tonic (F major) rather than the dominant (C major). The fourth eight-bar phrase is an exact repetition of the second. The second A section is a repeat of the first two eight-bar phrases of the beginning. The intervening B section is 12 bars long, divided into three four-bar groups. The first four bars are simply a repeated interval of a perfect 5th in the left hand. This *ostinato* will continue for the whole section. The remaining eight measures consist of a four-bar phrase in the right hand repeated twice. The second differs from the first only on the final two notes, preparing the recapitulation of the A section.

In terms of tempi, the B section is indicated to be faster, with the marking *Poco più vivo* (a little livelier). The B section ends with a *ritardando* into the following A section. The *b* section ends with a *fermata* in measure 24, indicating an arbitrary elongation while the piece concludes with a two-measure long *ritardando*. Throughout, frequent markings prescribe emphasis of the third beat of each measure. This emphasis is in keeping with the mazurka style, an intentional thwarting of the listener’s expectation of first-beat emphasis.

Figure 6 shows the first ten measures of the musical score with annotations for the sections discussed above and the harmonic progression in Roman numerals below the staff. The harmonies are standard, in fact, they are essentially the same as those of Pachelbel’s *Canon*,

Allegro ma non troppo. (♩ = 132.)

I \mathcal{A} * V \mathcal{A} * vi \mathcal{A} * iii \mathcal{A} * IV \mathcal{A} *

I IV I V/V V \mathcal{A} * \mathcal{A} *

Figure 6: The first ten measures of Chopin’s Mazurka Op. 68, No. 3. The harmonic progression is indicated below the staff in Roman numerals. Sections are marked above the staff, e.g., A (a). Analysis by the authors. This image comes from the complete score published by Bote and Bock in 1880. This composition is in the public domain, and the score is freely available via the International Music Score Library Project.

familiar to many as “that song played at weddings.” These harmonies, combined with the rhythmic repetition suggests a further division of this and all analogous sections into three small groupings: two two-measure phrases, followed by a four-measure phrase.

As a performer, these harmonic, rhythmic, and structural analyses aid in interpretation. The performer needs to decide how to emphasize or deemphasize these demarcations with slight or overt tempo or dynamic alterations. In a live performance, she could use physical motion to further suggest a particular interpretation. She can choose to emphasize long phrases, in this case, phrases of eight measures, or the shorter sub-phrases. Because of the repetition of similar phrases, she may choose to emphasize the long phrase on the first occurrence and shorter sub-phrases later on for variety, for example. While the musical structure suggests such possible interpretations, the performer must make these choices on her own, and may even alter those decisions from performance to performance.

3.2 Archetypal performances

Here we will carefully investigate the interpretive decisions implied by our estimated model for three rather different performances. Figure 7 shows the inferred state sequence for recordings made by Joyce Hatto in 1993 and Sviatoslav Richter in 1976. The B section is shaded in gray to better illustrate the formal divisions discussed above.

Our estimated model suggests that these two performers are quite different from each other. Hatto maintains a constant tempo carefully, remaining in state 1 with the exception of four periods of deceleration. All four periods coincide with the most significant phrase endings: at the end of the A section at measure 32, the end of the B section at measure 48, at the end of the piece, and the minor transition from $b \rightarrow a$ in the first A section (measure 24). According to our inferred model, she never accelerates or uses the transitory stress state.

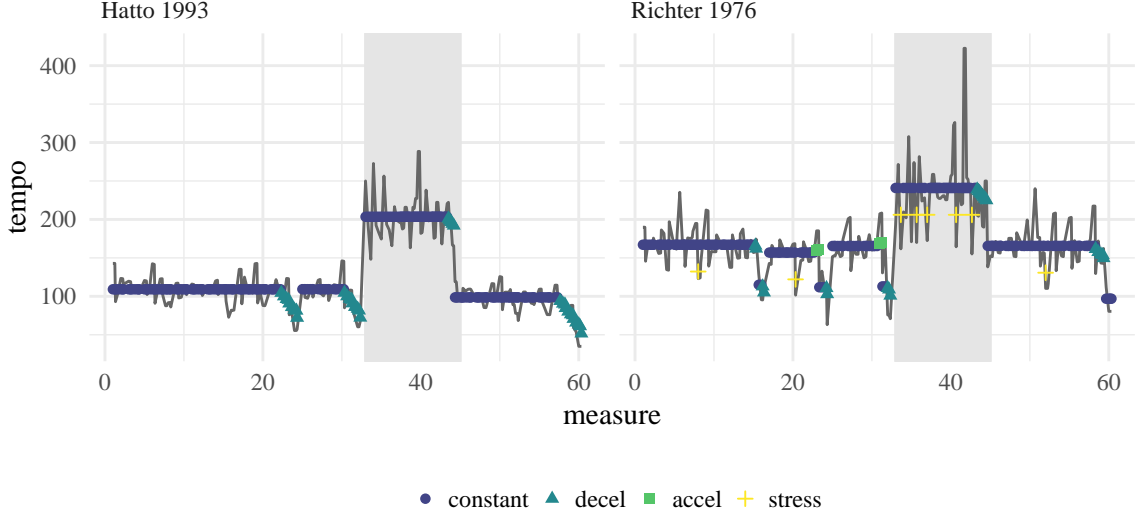


Figure 7: Inferred performer choices for two recordings.

Table 4: The estimated parameters for performances by Richter and Hatto.

	σ_ϵ^2	μ_{tempo}	μ_{acc}	μ_{stress}	σ_{tempo}^2	p_{11}	p_{12}	p_{22}	p_{31}	p_{13}	p_{21}	p_{32}
Richter 1976	426.70	136.33	-11.84	-34.82	439.38	0.85	0.05	0.74	0.44	0.02	0.25	0.17
Hatto 1993	405.57	130.36	-13.57	-27.93	408.99	0.94	0.03	0.82	0.36	0.01	0.16	0.19
Cortot 1951	403.71	182.84	-21.43	-45.67	460.82	0.92	0.02	0.71	0.34	0.03	0.23	0.09

In contrast, Richter uses all four states from our model. The short blips of acceleration before the B section and before the $b \rightarrow a$ transition are slightly out of place, and are likely better labelled as “constant”, but these state transitions describe more severe decelerations than the model’s linear assumption would allow (the multiplicative model in the Supplementary Material is much better). Richter uses stress frequently. Some may well be attributable to larger variance around constant tempo (picked up as frequent stress rather than larger σ_ϵ^2), but most correspond to interesting note emphases, for example the second beat of measure 20. This note is essentially a minor phrase ending, but it is also marked in the score with a *sforzando* (with sudden emphasis). It’s the first of two such occurrences in the piece, the second coming four measures later on the *fermata*, Richter’s slowest note in the entire piece. Richter likely chooses to make this prescribed emphasis with a sudden slow down in part because it takes place within the context of an already loud passage, precluding the use of extra volume. Table 4 shows the estimated parameters for these two performances.⁴ Richter has larger observation variance, σ_ϵ^2 , slightly faster average tempo, lower acceleration, and larger stress. He also has a larger tempo variance, meaning that returns to state 1 can start at relatively different tempos. On the other hand, Hatto is much more likely to remain in states 1 or 2. These inferences are largely consistent with the visual messages of Figure 7. The variability definitely increases around the constant tempo in Richter’s performance and

⁴In the Supplementary Material, we provide the estimates along with some measures of uncertainty for all 46 recordings.

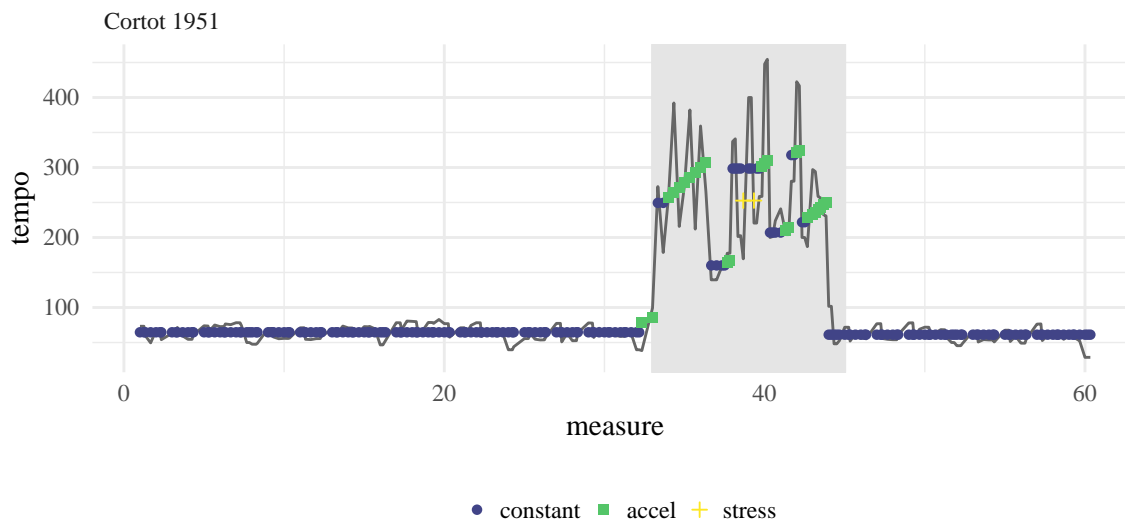


Figure 8: Inferred performance choices for Alfred Cortot’s 1951 recording.

he uses faster overall tempos in both the A and B sections. While these two performances are quite different from each other, they also display similarities. Both take a faster tempo in the B section versus the A sections. Both performers slow down at the end of the piece, at the end of the B section, immediately preceding the B section, and at the $b \rightarrow a$ transition.

Alfred Cortot’s 1951 performance is displayed in Figure 8. Both in terms of the parametric model we propose, and if we simply compare the vectors of note-by-note tempos (discussed in more detail below), this performance is an outlier. Cortot never uses the deceleration state, and he remains in constant tempo for the entirety of both A sections. While the model describes his performance well, it also illustrates a deficiency of this approach: Cortot, more than any other performer, has large contrasts between the A and B sections. His A section is the slowest of all 46 recordings at around 64 b.p.m., half the marked tempo. The next slowest is Maryla Jonas’s recording at around 84 b.p.m. Meanwhile, his B section is among the fastest of all the recordings and contains the fastest individual note. Additionally, there is stunningly little tempo variability in his A sections, but dramatic variation in the B section coupled with frequent uses of the acceleration and emphasis states. Taken together, Cortot’s performance may be better described by estimating our model separately on the two sections.⁵

3.3 Comparing performances

To better understand how the 46 recordings relate to each other, we measured the distance between their vectors of parameter estimates. Because the parameters have different scales, have different domains, and can covary, we use Mahalanobis distance to scale by the inverse of the prior covariance. That is, the distance between performance i and performance j is

⁵Cook (2013) suggests that this recording is not due to Cortot at all but part of a scandal at the Concert Artist label referred to as the “Hatto hoax”, wherein her husband, owner of the label, released over 100 recordings made by others but listing her as the performer.

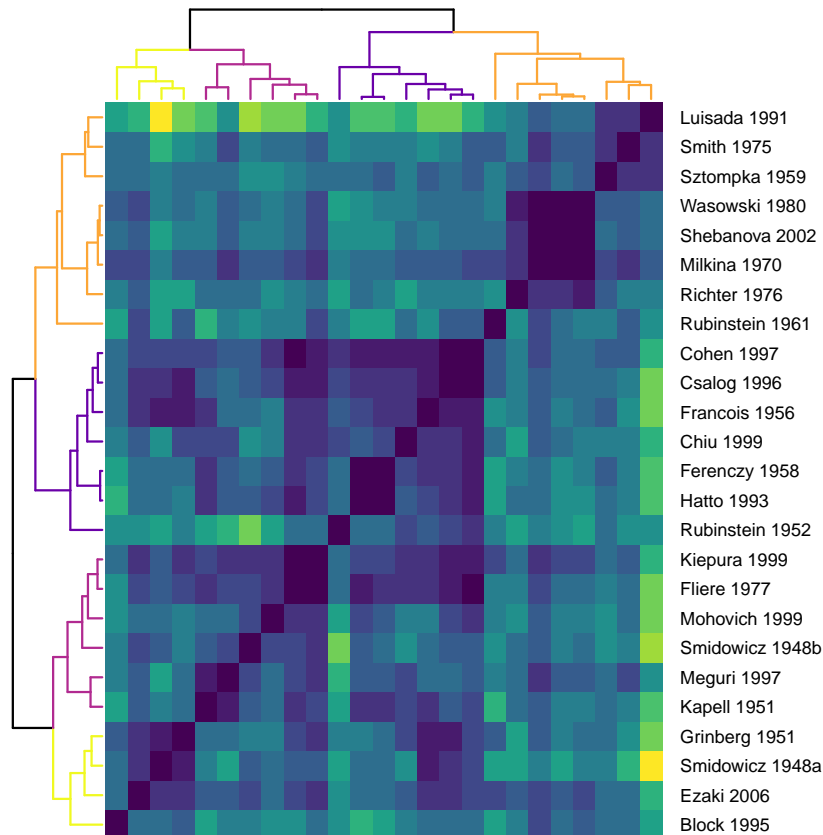


Figure 9: Distance matrix using the estimated parameters for all 46 performances.

given by

$$d_{i,j} = \left(\hat{\theta}_i - \hat{\theta}_j\right)^\top \Omega \left(\hat{\theta}_i - \hat{\theta}_j\right) \quad (3)$$

where $\hat{\theta}$ corresponds to the estimates in, e.g. Table 4, and the prior precision, $\Omega = \Sigma^{-1}$, is calculated based on the distributions in Table 3. We use the prior covariance rather than the covariance of the estimated parameters because any parameters that are poorly identified by the model will have small estimated variance, and therefore dominate the distance calculation. Using the prior avoids this pathology and while still properly accounting for scale and structural dependence.

Figure 9 shows the distance matrix calculated from the estimated parameters for all 46 performances. The dendrogram helps to visualize similarities between the performances, but should be taken only as a heuristic. Across a variety of clustering procedures, methods for choosing the number of clusters (e.g., Tibshirani et al., 2001; Dudoit and Fridlyand, 2002) consistently suggest that there is only one cluster. The procedure developed by Tibshirani et al. (2001) chooses the number of clusters by finding the first maximum of the Gap statistic, subject to a measure of uncertainty. For the Chopin performances, the global maximum occurs at 7 clusters, which is both implausible and not robust to uncertainty. Nonetheless, for the purposes of organizing this section, we will consider those performances within a “group” to be more similar than across groups.

In order to inspect these performances visually, we follow the advice of an anonymous

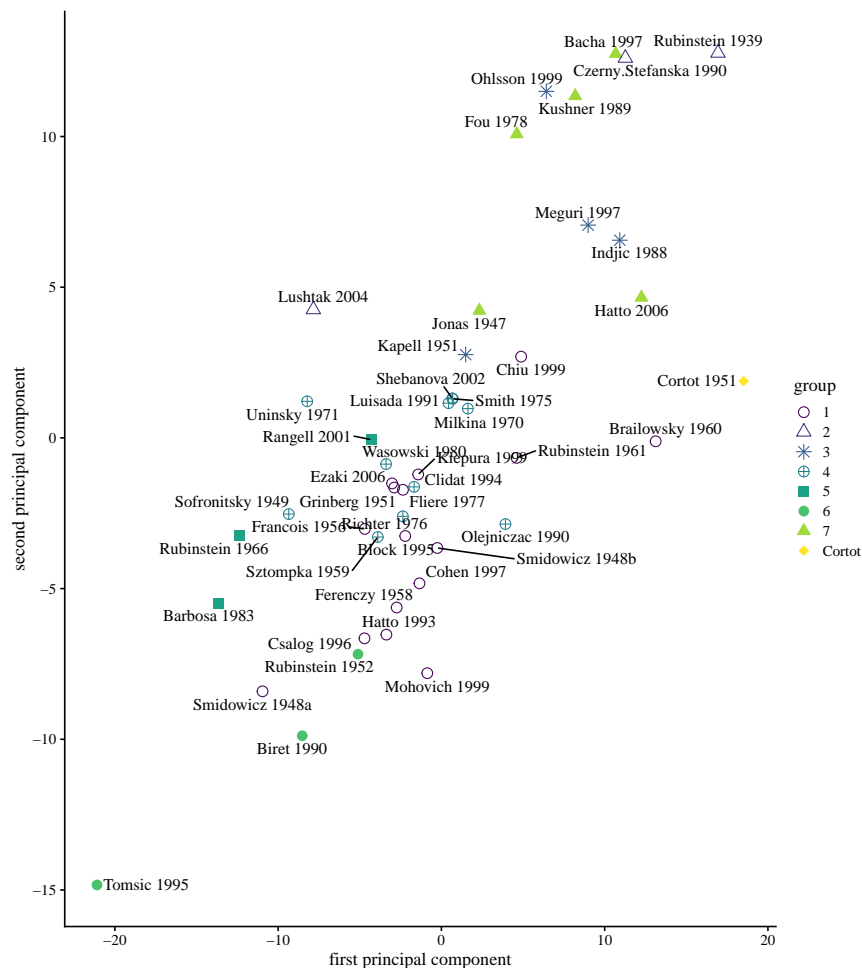


Figure 10: The first two principal components of the matrix of estimated parameters. Similar performances are indicated by shape.

reviewer and perform principal components analysis on the matrix of estimated parameters. Only about 45% of the variance is explained by the first 2 components, and we would need 7 to explain 90%, but Figure 10 nonetheless corresponds somewhat closely to the groups suggested by the dendrogram in Figure 9. In the Supplementary Material, we plot all the inferred performance decisions by group and give the factor loadings for the first few principal components. In the remainder of this section, we describe typical behaviors of the performances within a few groups that have relatively small within-group variability.

The first group (indicated as \circ in Figure 10) corresponds to reasonably staid performances. This group is the largest and corresponds to the block from Cohen to Brailowsky in Figure 9. In this group, the emphasis state is rarely visited with the performer tending to stay in the constant tempo state with periods of slowing down at the ends of phrases. Acceleration is almost never used. Furthermore, these performances have relatively slow average tempos, and not much difference between the A and B sections. Joyce Hatto’s recording in Figure 7 is typical of this group.

Recordings in the fourth group (\oplus in Figure 10) are those in the upper right of Figure 9, from Olejniczac to Richter. These recordings tend to transition quickly between states,

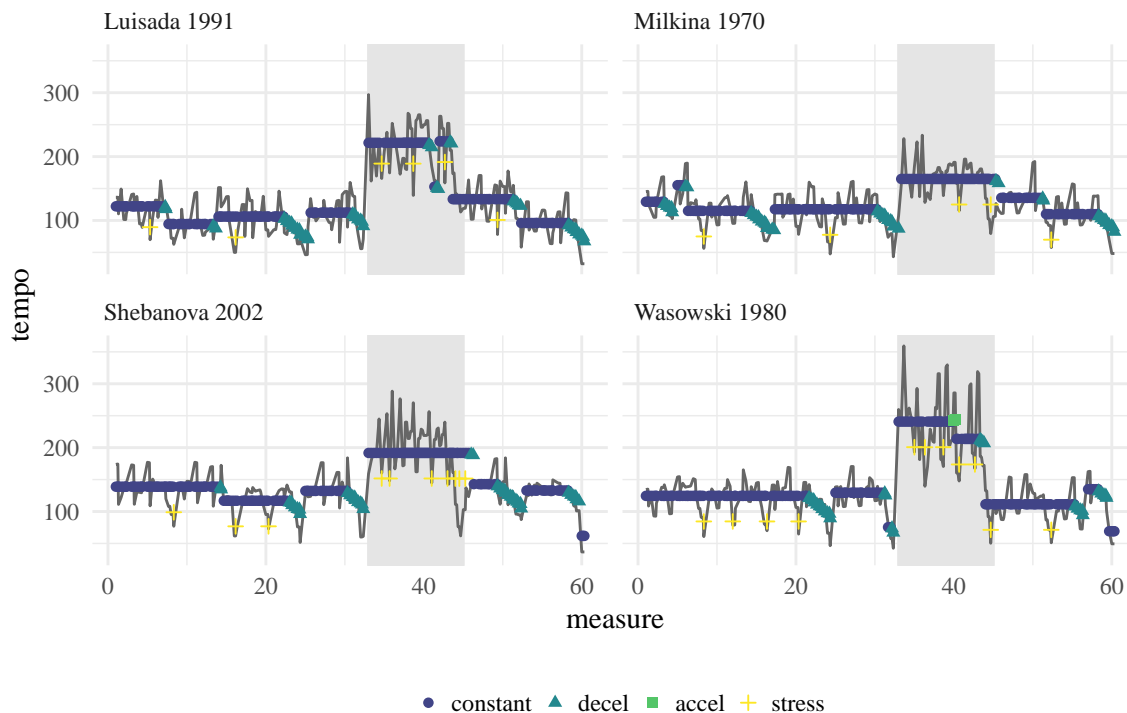


Figure 11: Four similar performances, all in the fourth group (\oplus).

especially constant tempo and slowing down, accompanied by frequent transitory emphases. The probability of remaining in state 1 is the lowest while the probability of entering state 2 from state 1 is the highest. The acceleration state is rarely visited. Four of the most similar performances are in this group, shown in Figure 11, along with Richter’s 1976 recording.

The three performances in group six (\bullet) are actually quite like others, but with small exceptions. Biret’s 1990 performance is very much like those in group 1, but with a much larger contrast between tempos in the A and B sections. The recording by Rubinstein in 1952 is similar, though with a faster A section that has less contrast with the B section. Tomsic’s 1995 performance is actually most similar to those in group three ($*$), but played much faster and with a large σ_ϵ^2 .

Comparing our groups to those we would find by applying the same procedure to the distances between note-by-note tempo vectors reveals a number of differences (see the Supplement (McDonald et al., 2021) for the distance matrix calculated in this way). The four similar recordings in Figure 11 would be spread across three different groups, for example, as would our group one. On the other hand, grouping by tempo vectors often (somewhat miraculously) groups recordings by the same pianist together: both recordings by Smidowicz (same as grouping by parameters), three of the four recordings by Rubinstein, and both recordings by Hatto. Both metrics see Cortot’s recording as a strong outlier (the remote \blacklozenge in Figure 10). In terms of Equation (3), Cortot’s recording is 1.7 times farther from its nearest neighbor than is the case for the next most dissimilar recording.

Figure 12 shows all four Rubinstein recordings. The 1939 recording is rather odd in that the measures 24–32 are so slow relative to the rest of the A section. The variability in the 1966 recording nearly obscures the contrast between the B section and the surrounding A

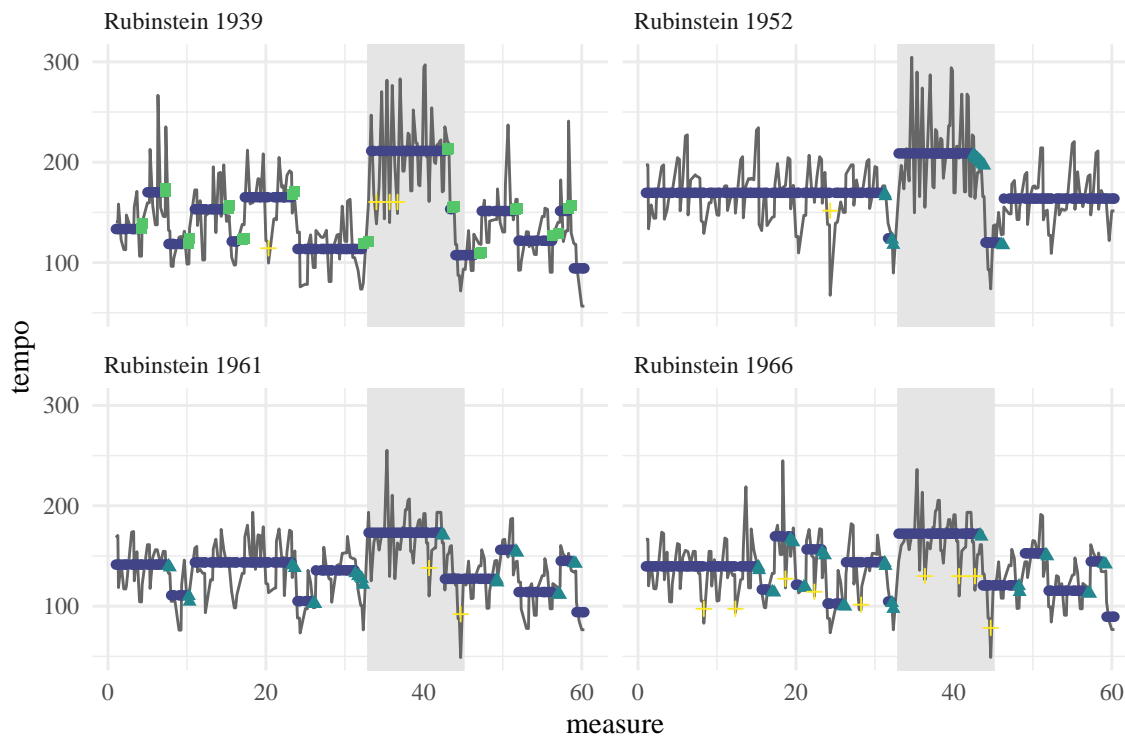


Figure 12: The four recordings by Arthur Rubinstein. Our clustering puts the 1952 and 1961 recordings in clusters one and two while leaving the others out. Clustering by tempo vector separates 1952 from the other three.

sections. These two recordings are nonetheless grouped together by the tempo vectors. Our method on the other hand, puts these four recordings in different groups. The estimated parameters for these four performances are shown in the bottom half of Table 5. The top half shows the parameters for the four similar performances in Figure 11. There is much larger variability across Rubinstein’s recordings, as we would expect.

3.4 Alternative smoothers

Our model is just one type of smoothing one could imagine using to find low-dimensional structure for the vector of note-by-note tempos. Alternative statistical techniques are common, and examining how they compare with our method helps to illuminate some of its benefits. The most obvious alternative is to use splines (Craven and Wahba, 1978; Wahba, 1990) though total-variation denoising or trend filtering (Kim et al., 2009; Tibshirani, 2014) are other reasonable alternatives. These statistical techniques perform smoothing by encouraging small changes in derivatives (splines) or bounded total variation (trend filtering). But musical performances do not conform to these assumptions because tempo interpretations rely on the juxtaposition of local smoothness with sudden changes and emphases to create listener interest. It is exactly the parts of a performance that are poorly described by statistical smoothers that render a performance interesting. Furthermore, many of these inflections are notated by the composer or are implicit in performance practice developed over centuries of musical expressivity. Consequently, smoothing that incorporates domain knowledge leads

Table 5: The estimated parameters for the four similar performances in group four and those for all four by Arthur Rubinstein.

	σ_ϵ^2	μ_{tempo}	μ_{acc}	μ_{stress}	σ_{tempo}^2	p_{11}	p_{12}	p_{22}	p_{31}	p_{13}	p_{21}	p_{32}
Wasowski 1990	414.99	132.00	-10.00	-40.00	425.00	0.85	0.05	0.67	0.34	0.02	0.26	0.2
Shebanova 2002	439.98	132.00	-10.00	-40.00	400.02	0.85	0.05	0.67	0.33	0.02	0.27	0.20
Richter 1976	426.70	136.33	-11.84	-34.82	439.38	0.85	0.05	0.74	0.44	0.02	0.25	0.17
Milkina 1970	435.25	136.38	-9.68	-40.02	400.01	0.87	0.05	0.68	0.33	0.02	0.26	0.21
Rubinstein 1939	520.32	145.26	-7.89	-50.82	345.64	0.89	0.02	0.83	0.56	0.05	0.13	0.16
Rubinstein 1952	481.13	128.13	-7.76	-17.59	409.30	0.93	0.04	0.68	0.32	0.01	0.28	0.19
Rubinstein 1961	434.23	139.17	-8.34	-35.08	355.00	0.90	0.06	0.56	0.46	0.01	0.41	0.19
Rubinstein 1966	380.95	127.24	-8.80	-42.28	473.69	0.87	0.07	0.36	0.34	0.01	0.61	0.20

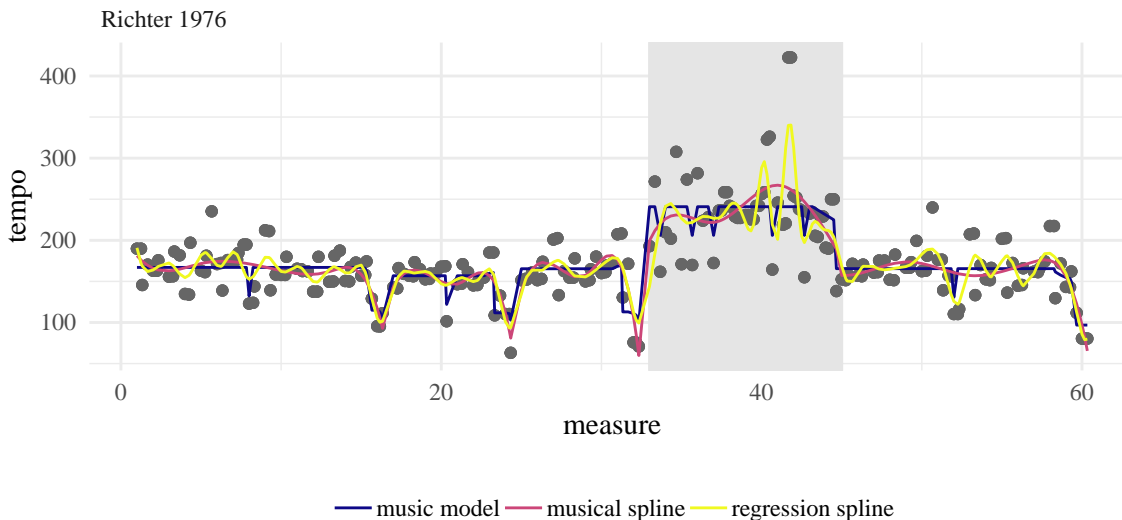


Figure 13: Smoothing with splines and musical models

to better statistical and empirical results.

Figure 13 shows the note-by-note tempo of Richter’s 1976 recording. Regression splines with equally spaced knots are shown with a dashed line. We use generalized cross validation (Golub et al., 1979) to select the number of knots (one knot per measure). The dotted line shows a regression spline fewer knots, but whose locations were chosen manually to coincide with the musical phrase endings discussed in Section 3.1. Knots at phrase endings were duplicated up to four times to allow for discontinuities. The solid line shows the estimated smooth tempo from our model (the same as in Figure 7). The regression spline with equally spaced knots undersmooths in constant tempo areas in an attempt to capture sudden emphases and dramatic changes in others. The spline with informed knot choice does much better, picking up the periods of deceleration at the ends of phrases. Our model learns these behaviors on its own while also capturing individual emphases that are missed in the musical analysis but are idiosyncratic to Richter’s playing. It is also more parsimonious to musical interpretation, inferring constant tempo periods rather than resulting in smoothly varying

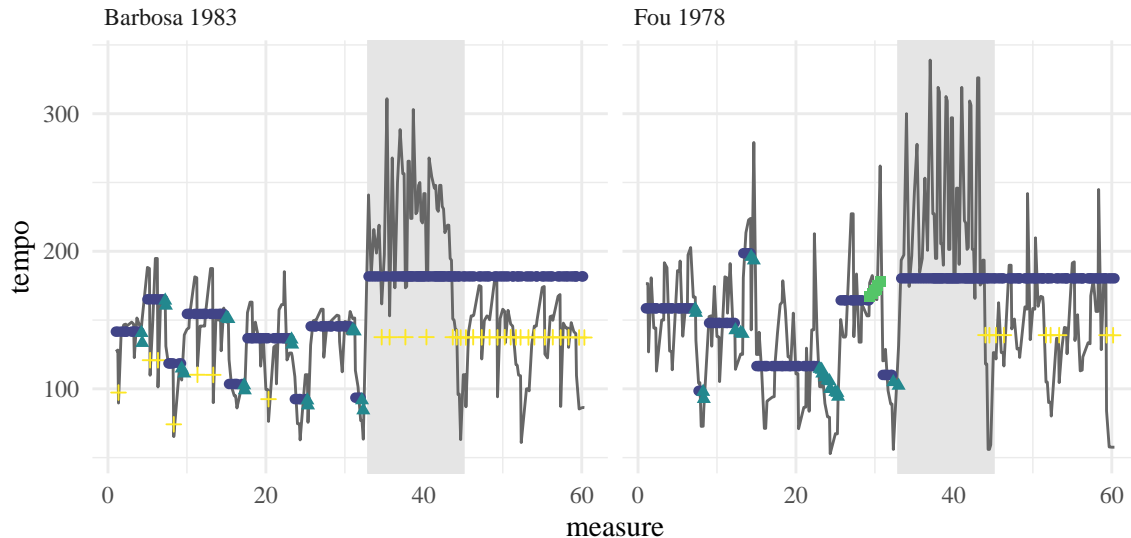


Figure 14: Estimation errors on two performances.

tempos in stable periods.

3.5 Problems with the model and estimation

While our model of musical decision making yields interesting insights into performance practice most of the time, it also suffers from some deficiencies. As discussed above in reference to Alfred Cortot’s recording, the assumption that all parameters are stable over the entire piece may not always be accurate. The μ_{tempo} parameter especially, should be estimated separately in different sections. This problem will only be compounded in more complex music with many contrasting sections. A related issue is the current form for the slowing down and speeding up sections. Our model assumes that both occur linearly, with a constant decrease of μ_{acc} b.p.m. An ability to slow increasingly as one remains in the state may improve the model fit. The multiplicative model described in more detail in the Supplementary Material addresses this issue but requires further work.

There is nothing intrinsic to the model which forces states 2, 3, or 4 to always go in the correct direction. If for example, μ_{acc} is small in magnitude relative to σ_{acc}^2 , a purposeful acceleration could be explained as time spent in state 2 but with large positive errors. For this piece, the priors help to avoid such occurrences, but this aspect of the Gaussian state-space model could be improved by enforcing non-Gaussian behavior. Of course, such constraints would complicate likelihood evaluation since the Kalman filter could no longer be used.

Relatedly, our model produced objectively incorrect inferences on two performances (Figure 14). Here, the estimated path failed to transition to state 1 at the recapitulation of the A section. In both cases, the resulting path stands out dramatically, remaining in the much faster constant tempo state from the B section with overly frequent emphases. Both of these performances are quite volatile, making estimation difficult. Altering the prior distributions along the lines suggested in the next section may help.

3.6 Prior sensitivity and generalization

As discussed in [Section 2.4](#), the main reason for the prior distributions shown in [Table 3](#) is that they help to identify the parameters. It is this identifiability issue that mainly guided our choices. For instance, if μ_{stress} is too similar to μ_{acc} , then a sequence like $1 \rightarrow 4 \rightarrow 1 \rightarrow 1$ will be hard to distinguish from $1 \rightarrow 2 \rightarrow 2 \rightarrow 1$. So, while it is important that those priors have low probability on common support, their shapes are less important for inference. Similar arguments hold for the other parameters.

With this intuition in mind, these priors should allow the model to work reasonably on similar piano pieces, even from different eras (Baroque, Classical, Modernist). That said, the specific values of prior means (for example, 10 for μ_{acc}) would be better expressed relative to the overall average speed, perhaps as $\bar{Y}/10$ b.p.m. or similar. In this way, really slow or fast pieces could be more easily accommodated. Since we only looked at one score, it is sufficient to simply fix some values. Using these 4 states should be enough for many types of music, even beyond piano recordings. However, music with more sections, say a piano sonata or a Prelude by Claude Debussy, would likely benefit from the inclusion of more discrete states. Adding another layer to [Figure 2](#) that can handle formal divisions is one such option, while employing a Dirichlet process similar to that used by [Ren et al. \(2010\)](#) may also work.

To gauge prior sensitivity (subject to the constraints above), we also estimated the model under alternative specifications. In particular we examine Sviatoslav Richter’s 1976 performance under four alternative priors: (1) replacing all Gamma distributions with inverse Gamma to examine the influence of tail shape; (2) making σ_c^2 smaller; (3) setting $p(\sigma_c^2) = p(\sigma_{\text{tempo}}^2) \propto 1$; (4) replacing the informative transition probability priors with uniform distributions. We calculate the root-mean squared error (RMSE) and the negative log likelihood under different choices. The results are roughly similar both in terms of quantitative metrics and the qualitative inferences based on the figures. The most different setting occurs for choice (2) which decreases the quality of the fit, eliminates the use of the “emphasis” state, and has trouble dealing with the faster B section. A more comprehensive evaluation of these prior choices is included in the Supplement where we show the specific distributions and the inferred performance decisions (like in [Figure 7](#)) under each choice.

4 Discussion

Musical interpretation is the most important factor in determining whether or not concertgoers enjoy a classical performance. Every performance includes mistakes—intonation issues, a lost note, an unpleasant sound—but these are all easily forgotten (or unnoticed) when a performer engages her audience, imbuing a piece with novel emotional content beyond the vague instructions inscribed on the printed page. While music teachers use imagery or heuristic guidelines to motivate interpretive decisions, combining these vague instructions to create a convincing performance remains the domain of the performer, subject to the whims of the moment, technical fluency, and taste.

In this paper, we develop a statistical model for tempo to elucidate performance decisions from classical music recordings. We present an algorithm for performing likelihood inference, estimate our model using a large collection of recordings of the same composition, and demonstrate how the model is able to recover performer intentions, and how they relate to standard

musical analysis. While our methods perform well, our analysis reveals a number of avenues for future work and improvement. For the piano, apart from tempo decisions, the performer can also control dynamics differentially. Similar techniques to those employed here could be used to describe levels of loudness, and creating a model that combined both is desirable. Pianists have relatively few variables under their control for interpretation: tempo, dynamics, and pedalling. On the other hand, string players have many more. Bowing decisions, fingerings, vibrato, and broken chords are all important tools which are difficult to discern aurally from a recording, let alone describe with a simple statistical model. Significant work would be required to generalize our techniques to more detailed interpretative analysis. Examining more complex genres—sonatas, string quartets, symphonies—would also be interesting for future work.

Another avenue we wish to pursue in the future is to examine how our model’s implications may be useful for teaching students. Can we estimate it quickly to provide immediate feedback to novice pianists? In this paper, we used a dataset in which the note-by-note tempos were annotated by experienced musicians. Combining our model with existing approaches to solving the note-score alignment problem ([Lang and Freitas, 2005](#); [Raphael, 2002](#); [Dannenberg and Raphael, 2006](#)), perhaps to their benefit would be the first step. Together, this could produce an immediate graphical representation that students and teachers could use to evaluate and improve their practice.

Acknowledgements

DJM was partially supported by the National Science Foundation Grant Nos. DMS-1407439 and DMS-1753171. CR was partially supported by National Science Foundation Grants IIS-1526473 and IIS-0812244.

References

- Anderson, B. D. and Moore, J. B. (1979) *Optimal filtering*. Englewood Cliffs, NJ: Prentice-Hall. 7, 33
- Andrieu, C., Doucet, A. and Holenstein, R. (2010) Particle Markov chain Monte Carlo methods. *Journal of the Royal Statistical Society. Series B, Statistical Methodology*, **72**, 1–33. 7
- Arcos, J. and Mantaras, R. L. (2001) An interactive cbr approach for generating expressive music. *Journal of Applied Intelligence*, **21**, 115–129. 4
- Ariza, C. (2005) Navigating the landscape of computer aided algorithmic composition systems: a definition, seven descriptors, and a lexicon of systems and research. In *Proceedings of International Computer Music Conference*. 4
- Arzt, A. and Widmer, G. (2015) Real-time music tracking using multiple performances as a reference. In *International Society for Music Information Retrieval (ISMIR)*, 357–363. 4
- Bernstein, L. (2005) *Young People’s Concerts*. Pompton Plains, NJ: Amadeus Press. 2
- Bisiani, R. (1992) Beam search. In *Encyclopedia of Artificial Intelligence* (ed. S. Shapiro). John Wiley and Sons, 2nd edn. 12
- Block, B. A., Jonsen, I. D., Jorgensen, S. J., Winship, A. J., Shaffer, S. A., Bograd, S. J., Hazen, E. L., Foley, D. G., Breed, G., Harrison, A.-L. et al. (2011) Tracking apex marine predator movements in a dynamic ocean. *Nature*, **475**, 86. 7
- Boulanger-Lewandowski, N., Bengio, Y. and Vincent, P. (2012) Modeling temporal dependencies in high-dimensional sequences: Application to polyphonic music generation and transcription. In *Proceedings of the 29th International Conference on Machine Learning*. Edinburgh, Scotland, UK. 4
- Bresin, R., Friberg, A. and Sundberg, J. (2002) Director musices: The KTH performance rules system. In *Proceedings of SIGMUS-46*. Kyoto. 4
- Burkholder, J. P., Grout, D. J. and Palisca, C. V. (2014) *A History of Western Music*. WW Norton & Company, 9th edn. 15
- CHARM (2009) Centre for the History and Analysis of Recorded Music. URL: <http://www.charm.rhul.ac.uk/about/about.html>. Online; accessed 12 March 2019. 6
- Collins, N. (2016) A funny thing happened on the way to the formula: Algorithmic composition for musical theater. *Computer Music Journal*, **40**, 41–57. 4
- Cont, A. (2010) A coupled duration-focused architecture for real-time music-to-score alignment. *IEEE Transactions on Pattern Analysis and Machine Intelligence*, **32**, 974–987. 4

- Cont, A., Schwarz, D., Schnell, N. and Raphael, C. (2007) Evaluation of real-time audio-to-score alignment. In *International Symposium on Music Information Retrieval (ISMIR)*. 4
- Cook, N. (2013) *Beyond the score: Music as performance*. Oxford University Press. 18
- Craven, P. and Wahba, G. (1978) Smoothing noisy data with spline functions. *Numerische Mathematik*, **31**, 377–403. 22
- Dannenberg, R. (1985) An on-line algorithm for real-time accompaniment. In *Proceedings of the 1984 International Computer Music Conference*, 193–198. International Computer Music Association. 4
- Dannenberg, R. B. and Raphael, C. (2006) Music score alignment and computer accompaniment. *Communications of the ACM*, **49**, 38–43. 4, 26
- Dror, G., Koenigstein, N., Koren, Y. and Weimer, M. (2012) The Yahoo! Music Dataset and KDD-Cup’11. In *KDD Cup*, 8–18. 2
- Dudoit, S. and Fridlyand, J. (2002) A prediction-based resampling method for estimating the number of clusters in a dataset. *Genome Biology*, **3**, research0036.1. 19
- Durbin, J. and Koopman, S. (2001) *Time Series Analysis by State Space Methods*. Oxford: Oxford Univ Press. 7
- Durbin, J. and Koopman, S. J. (1997) Monte Carlo maximum likelihood estimation for non-Gaussian state space models. *Biometrika*, **84**, 669–684. 7
- Earis, A. (2007) An algorithm to extract expressive timing and dynamics from piano recordings. *Musicae Scientiae*, **11**, 155–182. 4, 6
- (2009) Mazurka in F Major, Op. 68, No. 3. URL: <http://mazurka.org.uk/auto/earis/mazurka68-3/>. Accessed 12 March 2019. 6
- Eddelbuettel, D. (2013) *Seamless R and C++ Integration with Rcpp*. New York: Springer. 15
- Fearnhead, P. and Clifford, P. (2003) On-line inference for hidden markov models via particle filters. *Journal of the Royal Statistical Society: Series B (Statistical Methodology)*, **65**, 887–899. 12
- Flossman S. Grachten, M. and Widmer, G. (2012) Expressive performance rendering with probabilistic models. In *Guide to Computing for Expressive Music Performance* (eds. A. Kirke and E. Miranda). Springer. 4, 5
- Flossmann, S., Grachten, M. and Widmer, G. (2013) Expressive performance rendering with probabilistic models. In *Guide to Computing for Expressive Music Performance*, 75–98. Springer. 4

- Forsén, S., Gray, H. B., Lindgren, L. O. and Gray, S. B. (2013) Was something wrong with Beethoven’s metronome? *Notices of the AMS*, **60**, 8
- Fox, E. B., Sudderth, E. B., Jordan, M. I. and Willsky, A. S. (2011) A sticky HDP-HMM with application to speaker diarization. *The Annals of Applied Statistics*, **5**, 1020–1056. 7
- Fuh, C.-D. (2006) Efficient likelihood estimation in state space models. *Annals of Statistics*, **34**, 2026–2068. 7
- Ghahramani, Z. and Hinton, G. E. (2000) Variational learning for switching state-space models. *Neural Computation*, **12**, 831–864. 7, 12
- Golub, G. H., Heath, M. and Wahba, G. (1979) Generalized cross-validation as a method for choosing a good ridge parameter. *Technometrics*, **21**, 215–223. 23
- Grindlay, G. and Helmbold, D. (2006) Modeling, analyzing, and synthesizing expressive piano performance with graphical models. *Machine Learning*, **65**, 361–387. 4, 5
- Gu, Y. and Raphael, C. (2012) Modeling piano interpretation using switching Kalman filter. In *International Society for Music Information Retrieval (ISMIR)*, 145–150. 13, 14, 37, 38
- Hadjeres, G., Pachet, F. and Nielsen, F. (2017) DeepBach: a steerable model for Bach chorales generation. In *Proceedings of the 34th International Conference on Machine Learning* (eds. D. Precup and Y. W. Teh), vol. 70 of *Proceedings of Machine Learning Research*, 1362–1371. International Convention Centre, Sydney, Australia: PMLR. 4
- Hamilton, J. (2011) Calling recessions in real time. *International Journal of Forecasting*, **27**, 1006–126. 7
- Harvey, A. C. (1990) *Forecasting, structural time series models and the Kalman filter*. Cambridge University Press. 6
- Kallberg, J. (1996) *Chopin at the boundaries: Sex, history, and musical genre*. Harvard University Press. 15
- Kalman, R. E. (1960) A new approach to linear filtering and prediction problems. *Journal of Basic Engineering*, **82**, 35–45. 6
- Kim, C. and Nelson, C. (1998) Business cycle turning points, a new coincident index, and tests of duration dependence based on a dynamic factor model with regime switching. *Review of Economics and Statistics*, **80**, 188–201. 7
- Kim, C.-J. (1994) Dynamic linear models with markov-switching. *Journal of Econometrics*, **60**, 1–22. 7
- Kim, S.-J., Koh, K., Boyd, S. and Gorinevsky, D. (2009) ℓ_1 trend filtering. *SIAM Review*, **51**, 339–360. 22
- Kitagawa, G. (1987) Non-Gaussian state-space modeling of nonstationary time series. *Journal of the American Statistical Association*, **82**, 1032–1041. 7

- (1996) Monte Carlo filter and smoother for non-Gaussian nonlinear state space models. *Journal of Computational and Graphical Statistics*, 1–25. 7
- Koyama, S., Pérez-Bolde, L. C., Shalizi, C. R. and Kass, R. E. (2010) Approximate methods for state-space models. *Journal of the American Statistical Association*, **105**, 170–180. 7
- Lang, D. and Freitas, N. D. (2005) Beat tracking the graphical model way. In *Advances in Neural Information Processing Systems*, 745–752. Cambridge, MA: MIT press. 26
- Lang, M., Bischl, B. and Surmann, D. (2017) batchtools: Tools for R to work on batch systems. *The Journal of Open Source Software*, **2**, 135. 15
- Maezawa, A. (2019) Deep linear autoregressive model of interpretable prediction of expressive tempo. In *Proceedings of the 16th Sound and Music Computing Conference*. Málaga, Spain. 4, 5
- McDonald, D. J., McBride, M., Gu, Y. and Raphael, C. (2021) Supplement to "Markov-switching state space models for uncovering musical interpretation". URL: <https://doi.org/10.1214/21-AOAS1457SUPPA>, <https://doi.org/10.1214/21-AOAS1457SUPPB>, <https://doi.org/10.1214/21-AOAS1457SUPPC>. 6, 7, 14, 21
- McFee, B. and Lanckriet, G. (2011) Learning multi-modal similarity. *Journal of Machine Learning Research*, **12**, 491–523. 4
- Mead, A. (2007) On tempo relations. *Perspectives of New Music*, **45**, 64–108. 14, 38
- van den Oord, A., Dieleman, S. and Schrauwen, B. (2013) Deep content-based music recommendation. In *Advances in Neural Information Processing Systems 26* (eds. C. J. C. Burges, L. Bottou, M. Welling, Z. Ghahramani and K. Q. Weinberger), 2643–2651. Curran Associates, Inc. 4
- Patterson, T. A., Thomas, L., Wilcox, C., Ovaskainen, O. and Matthiopoulos, J. (2008) State-space models of individual animal movement. *Trends in ecology & evolution*, **23**, 87–94. 7
- R Core Team (2019) *R: A Language and Environment for Statistical Computing*. R Foundation for Statistical Computing, Vienna, Austria. URL: <https://www.R-project.org/>. 15
- Raphael, C. (2002) A hybrid graphical model for rhythmic parsing. *Artificial Intelligence*, **137**, 217–238. 26
- (2010) Music plus one and machine learning. In *Proceedings of the 27th International Conference on Machine Learning (ICML-10)* (eds. J. Fürnkranz and T. Joachims), 21–28. Haifa, Israel. 4
- Rauch, H. E., Striebel, C. and Tung, F. (1965) Maximum likelihood estimates of linear dynamic systems. *AIAA journal*, **3**, 1445–1450. 7, 33

- Ren, L., Dunson, D., Lindroth, S. and Carin, L. (2010) Dynamic nonparametric Bayesian models for analysis of music. *Journal of the American Statistical Association*, **105**, 458–472. [4](#), [25](#)
- Roberts, A., Engel, J., Raffel, C., Hawthorne, C. and Eck, D. (2018a) A hierarchical latent vector model for learning long-term structure in music. In *Proceedings of the 35th International Conference on Machine Learning* (eds. J. Dy and A. Krause), vol. 80 of *Proceedings of Machine Learning Research*, 4364–4373. Stockholmsmässan, Stockholm Sweden: PMLR. [4](#)
- Roberts, A., Hawthorne, C. and Simon, I. (2018b) Magenta.js: A javascript api for augmenting creativity with deep learning. In *Joint Workshop on Machine Learning for Music (ICML)*. [4](#)
- Schedl, M., Gómez, E., Urbano, J. et al. (2014) Music information retrieval: Recent developments and applications. *Foundations and Trends® in Information Retrieval*, **8**, 127–261. [4](#)
- Stowell, D. and Chew, E. (2012) Bayesian MAP estimation of piecewise arcs in tempo time series. In *Proceedings of Computer Music Multidisciplinary Research*. [5](#)
- Sturm, B. L., Ben-Tal, O., Monaghan, Ú., Collins, N., Herremans, D., Chew, E., Hadjeres, G., Deruty, E. and Pachet, F. (2019) Machine learning research that matters for music creation: A case study. *Journal of New Music Research*, **48**, 36–55. [4](#)
- Thickstun, J., Harchaoui, Z. and Kakade, S. M. (2017) Learning features of music from scratch. In *International Conference on Learning Representations (ICLR)*. [4](#)
- Tibshirani, R., Walther, G. and Hastie, T. (2001) Estimating the number of clusters in a data set via the gap statistic. *Journal of the Royal Statistical Society. Series B (Statistical Methodology)*, **63**, 411–423. [19](#)
- Tibshirani, R. J. (2014) Adaptive piecewise polynomial estimation via trend filtering. *Annals of Statistics*, **42**, 285–323. [22](#)
- Vercoe, B. (1984) The synthetic performer in the context of live performance. In *Proceedings of the 1984 International Computer Music Conference*, 199–200. International Computer Music Association. [4](#)
- Wahba, G. (1990) *Spline models for observational data*, vol. 59 of *CBMS-NSF Regional Conference Series in Applied Mathematics*. Philadelphia, PA: Society for Industrial and Applied Mathematics (SIAM). [22](#)
- Whiteley, N., Andrieu, C. and Doucet, A. (2010) Efficient Bayesian inference for switching state-space models using discrete particle Markov chain Monte Carlo methods. *Tech. Rep. 10:04*, Bristol University. [12](#)
- Wickham, H. (2016) *ggplot2: Elegant graphics for data analysis*. Springer, 2nd edn. [15](#)

— (2017) *tidyverse: Easily Install and Load the ‘Tidyverse’*. URL: <https://CRAN.R-project.org/package=tidyverse>. R package version 1.2.1. 15

Widmer, G., Flossmann, S. and Grachten, M. (2009) YQX plays chopin. *AI Magazine*, **30**, 35. 4

A Supplementary material

A.1 Algorithms

For completeness, we include here concise descriptions of the Kalman filter and smoother we employ as inputs to our main algorithm. The filter is given in [Algorithm 2](#).

Algorithm 2 Kalman filter: estimate x_i conditional on $\{y_j\}_{j=1}^i$, for all $i = 1, \dots, n$ and calculate the log likelihood for θ

Input: Y, x_0, P_0, d, T, c, Z , and G

$\ell(\theta) \leftarrow 0$ ▷ Initialize the log-likelihood

for $i = 1$ to n **do**

$\mathcal{X}_i \leftarrow d + T x_{i-1|i-1}, P_i \leftarrow Q + T P_{i-1|i-1} T^\top$ ▷ Predict current state

$\tilde{y}_i \leftarrow c + Z \mathcal{X}_i, F_i \leftarrow G + Z P_i Z^\top$ ▷ Predict current observation

$v_i \leftarrow y_i - \tilde{y}_i, K_i \leftarrow P_i Z^\top F_i^{-1}$ ▷ Forecast error and Kalman gain

$x_{i|i} \leftarrow \mathcal{X}_i + K_i v_i, P_{i|i} \leftarrow P_i - P_i Z^\top K_i$ ▷ Update

$\ell(\theta) = \ell(\theta) - v_i^\top F_i^{-1} v_i - \log(|F_i|)$

end for

return $\tilde{Y} = \{\tilde{y}_i\}_{i=1}^n, \mathcal{X} = \{\mathcal{X}_i\}_{i=1}^n, \tilde{X} = \{x_{i|i}\}_{i=1}^n, P = \{P_i\}_{i=1}^n, \tilde{P} = \{P_{i|i}\}_{i=1}^n, \ell(\theta)$

To incorporate all future observations into these estimates, the Kalman smoother is required. There are many different smoother algorithms tailored for different applications. [Algorithm 3](#), due to [Rauch et al. \(1965\)](#), is often referred to as the classical fixed-interval smoother ([Anderson and Moore, 1979](#)). It produces only the unconditional expectations of the hidden state $\hat{x}_i = E[x_i | y_1, \dots, y_n]$ for the sake of computational speed. This version is more appropriate for inference in the type of switching models we discuss in the manuscript.

Algorithm 3 Kalman smoother (Rauch-Tung-Striebel): estimate \hat{X} conditional on Y

Input: $\mathcal{X}, \tilde{X}, P, \tilde{P}, T, c, Z$.

$i = n,$

$\hat{x}_n \leftarrow \tilde{x}_n,$

while $t > 1$ **do**

$\hat{y}_i \leftarrow c + Z \hat{x}_i,$ ▷ Predict observation vector

$e \leftarrow \tilde{x}_i - \mathcal{X}_i, V \leftarrow P_i^{-1},$

$i \leftarrow i - 1,$ ▷ Increment

$\hat{x}_i = \tilde{x}_i + \tilde{P}_i T V e$

end while

return $\hat{Y} = \{\hat{y}_i\}_{i=1}^n, \hat{X} = \{\hat{x}_i\}_{i=1}^n$

A.2 Principal components

In [Section 3.3](#) of the manuscript, [Figure 10](#) showed the first two principal components along with some notion of groups to gauge the similarities between performances. That figure is reproduced in color as [Figure 15](#).

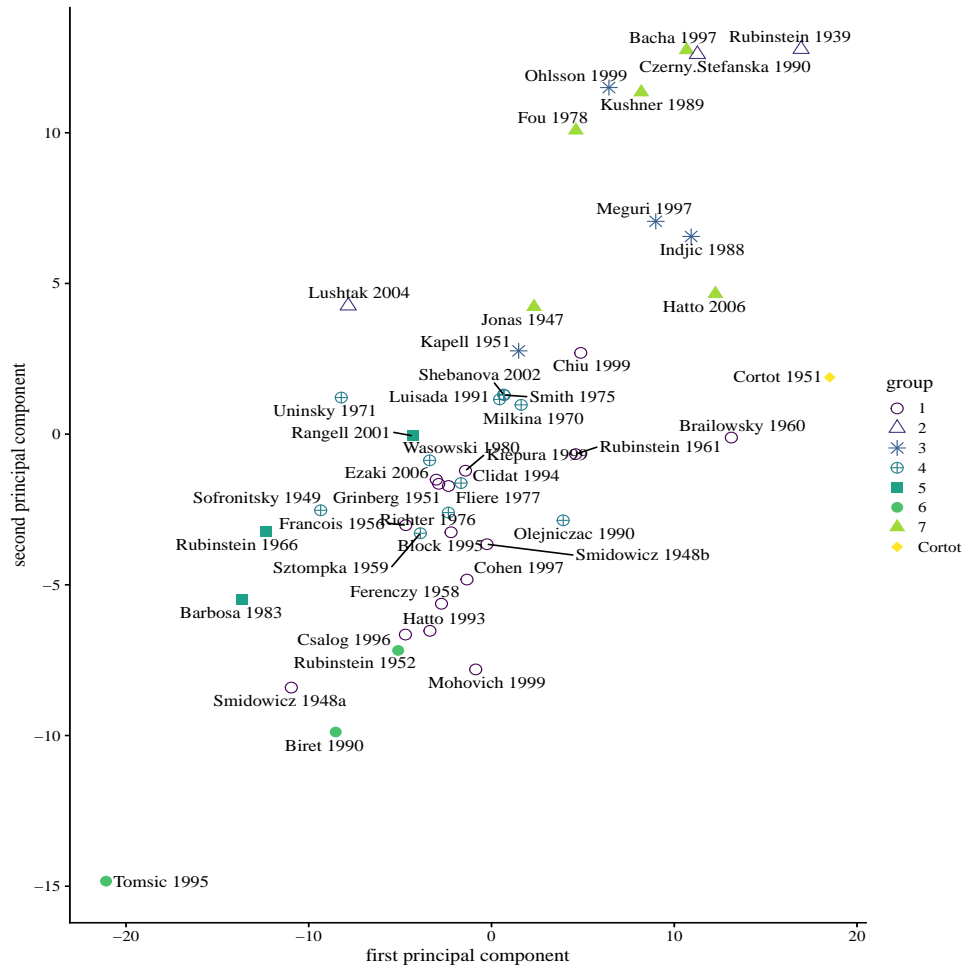


Figure 15: The first two principal components of the matrix of estimated parameters. Similar performances are indicated by shape/color. This is the same as Figure 10 in the manuscript.

Table 6: The factor loadings for principal component analysis of the parameter estimates.

	σ_ϵ^2	μ_{tempo}	μ_{acc}	μ_{stress}	σ_{tempo}^2	p_{11}	p_{12}	p_{31}	p_{13}	p_{21}	p_{32}	p_{22}
PC1	0.07	0.34	-0.66	-0.22	-0.09	0.27	-0.34	0.32	0.03	-0.05	-0.3	-0.05
PC2	0.07	0.00	-0.12	-0.48	-0.02	-0.46	0.13	-0.01	0.17	0.68	0.0	-0.17
PC3	0.64	-0.59	0.16	0.02	-0.03	0.08	-0.13	0.32	0.03	0.05	-0.3	-0.02

For additional context, [Table 6](#) gives the loadings for the first three principal components. We see that the first component picks up information about the first two states, both through μ_{tempo} and μ_{acc} as well as loading onto the probabilities p_{11} , p_{12} , and p_{31} . The second component loads especially onto μ_{stress} but also p_{11} and p_{21} . Finally, the third component loads mainly onto the observation error with smaller contributions from p_{31} .

A.3 Confidence intervals

[Section 3](#) of the manuscript includes parameter estimates for some of the recordings in our data set. In order to quantify uncertainty and compare the estimates, this section graphically displays all parameter estimates in [Figure 16](#). The recordings are sorted in the same order as in [Figure 9](#) in the main document, so some of the conclusions about groupings are readily apparent. The bars indicating measures of uncertainty are derived from the observed Fisher information from the optimization routine. However, it’s not entirely clear what these mean. For one, they ignore any uncertainty in the state sequence (see [Figure 27](#) some notion of the scale of this uncertainty). They also depend on identifiability, the priors, and the approximation to the posterior. Producing the MAP depends on the approximation accuracy at the MAP, but producing the Hessian needs that as well as the accuracy of about $5p^2$ additional function evaluations. And because we need the inverse, any inaccuracies could explode. The length of the confidence interval for parameter j is given by $4\sqrt{(\hat{I})_{jj}^{-1}}$ and so these would have roughly 95% coverage. For any parameters that are unidentified, the width of the band is the maximum over all performances for the same parameter. However, short of performing a fully-Bayesian analysis, we would hesitate to attach much certainty to these metrics of uncertainty.

A.4 Distance matrix from raw data

In [Section 3.3](#) of the manuscript, we present results for grouping performances using the low-dimensional vector of performance-specific parameters learned for our model. An alternative approach is to simply use the raw data, in this case, 231 individual note-by-note instantaneous speeds measured in beats per minute. In [Figure 17](#) we show the result of this analysis. A comparison between this clustering and that given by our model is discussed in some detail in the manuscript.

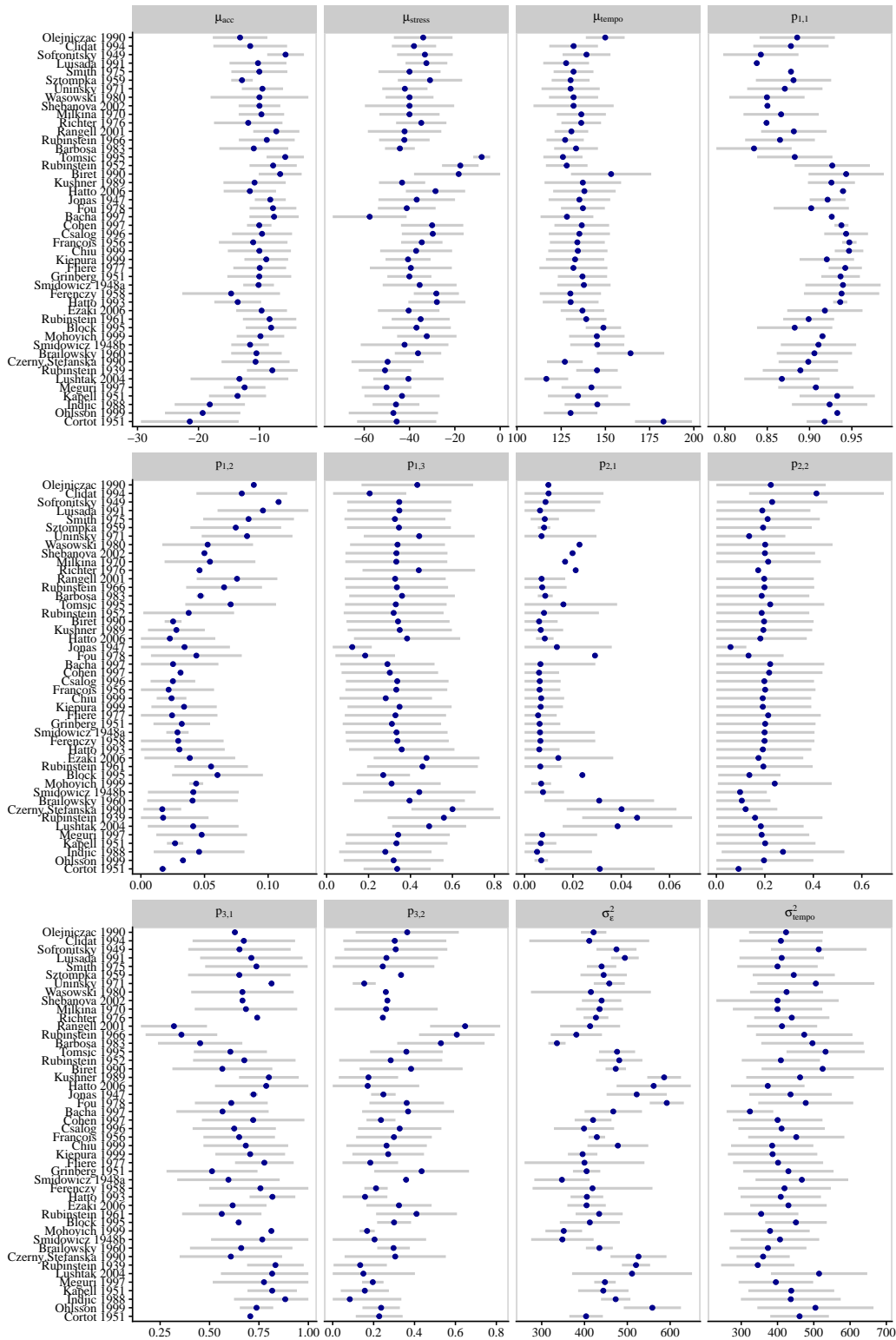


Figure 16: Confidence intervals for all parameters based on the observed Fisher information.

A.5 Plotting performances

Section 3.3 of the manuscript discusses 7 groups of recordings. Figures 18 to 24 display the note-by-note tempos along with the inferred interpretive decisions for all performances based on this grouping.

The first group (Figure 18 indicated as \circ in Figure 10) corresponds to reasonably staid performances. This group is the largest and corresponds to the block from Cohen to Brailowsky in Figure 9. In this group, the emphasis state is rarely visited with the performer tending to stay in the constant tempo state with periods of slowing down at the ends of phrases. Acceleration is almost never used. Furthermore, these performances have relatively slow average tempos, and not much difference between the A and B sections. Joyce Hatto’s recording in Figure 7 is typical of this group

Recordings in the fourth group (Figure 19, \oplus in Figure 10) are those in the upper right of Figure 9, from Olejniczak to Richter. These recordings tend to transition quickly between states, especially constant tempo and slowing down accompanied by frequent transitory emphases. The probability of remaining in state 1 is the lowest while the probability of entering state 2 from state 1 is the highest. The acceleration state is rarely visited. Four of the most similar performances are in this group along with Richter’s 1976 recording.

The three performances in group six (Figure 20, \bullet in Figure 10) are actually quite like others, but with small exceptions. Biret’s 1990 performance is very much like those in group 1, but with a much larger contrast between tempos in the A and B sections. The recording by Rubinstein in 1952 is similar, though with a faster A section that has less contrast with the B section. Tomsic’s 1995 performance is actually most similar to those in group three ($*$), but played much faster and with a large σ_ϵ^2 .

The remaining performances are displayed in Figures 21–24, with the exception of Cortot’s performance in the manuscript.

A.6 Investigation of oversmoothing

In Section 2.5 we argue that our model is not eliminating too much tempo information that would increase listener enjoyment. That is, we eliminate extraneous “noise” rather than beneficial “signal.” Gu and Raphael (2012) examine a related though simpler model and undertake an empirical investigation by asking experienced musicians to distinguish between recordings synthesized from their tempo model and actual performances. They find that listeners were not meaningfully able to distinguish between the two in the majority of experiments, suggesting that their model retains most of the “signal.” Our model is more expressive than theirs, and therefore even less likely to oversmooth. To examine this assertion, we compare the inferred tempo decisions for their model and ours for 3 performances.

Figure 25 shows the inferred tempo decisions for the model in this paper in the right column and those produced by Gu and Raphael (2012) on the left. We use the same prior distributions to estimate their model as described in the main document with minor adjustments to eliminate two probabilities from the Markov switching matrix. In the Luisada performance, our model is far more expressive, allowing for many more changes of tempo. This is most easily seen in the first A section where the Gu and Raphael (2012) model gets stuck in the constant tempo state, smoothing away all tempo information. It gets similarly

stuck in the Rubinstein recording, though there it appears to potentially have some additional flexibility, in the frequent use of the slowing-down state. Rather than using the linear “slowing down” behavior, our model begins a new constant tempo section in many of these passages.

To examine the amount of smoothing more specifically, [Figure 26](#) compares the cumulative sums of the absolute residuals over the recording relative to the cumulative sum of using the mean. A value of 1 here indicates a completely over-smoothed recording where we use the mean for a synthesized performance while a value of zero corresponds to the performed tempos. Clearly, in each case, the [Gu and Raphael \(2012\)](#) model smooths more than the model presented in this paper. Across all 46 performances, 35 are less smooth for our model, and the relative absolute residuals are smaller on average 0.506 vs 0.614.

A.7 Distribution over states

To examine the stability of the [Algorithm 1](#), we examined all the potential paths for Richter’s 1976 recording. Here, we saved the most likely 10,000 paths and their weights (rather than only the most likely path). [Figure 27](#) shows the marginal (posterior) probability of being in a particular state for each note. While the paper uses the most likely *path*, this figure is marginal in the sense that a particular note/state combination will have high probability when many paths visited that note/state. But, the most likely path may not have used that same note/state combination. Nonetheless, there appears to be consensus for many of the notes. The most obviously difficult notes are those near measures 10 and 50. In both cases, the most likely path ([Figure 1](#) in the main text) used the stress state, which exceeds 50% posterior probability here.

A.8 Multiplicative tempo changes

While an additive state space model is relatively easy to understand, some music theorists ([Mead, 2007](#), for example) have argued that musicians make multiplicative tempo adjustments. That is, it is the ratio between the tempo of the current note and that of the previous note rather than their difference that is important. Such a conception is fundamental to musical notation (quarter notes, eighth notes, etc) and frequently used to specify tempo changes within a piece of music, such as with $\downarrow = \downarrow$ to indicate that the next section should be played at half the previous tempo.

Rather than the linear switching model described in [Section 2](#), we examined the following multiplicative version:

$$\begin{aligned} x_1 &\sim \text{lognormal}(x_0, P_0), \\ \frac{x_{i+1}}{x_i} &= (1 - \mu(s_i))\eta_i, & \eta_i &\sim \text{lognormal}(0, Q(s_i)), \\ y_i &= c(s_i) + x_i + \epsilon_i, & \epsilon_i &\sim N(0, G(s_i)). \end{aligned}$$

Here, $\mu(s_i)$ is 0 in the constant tempo or emphasis states and controls the magnitude of acceleration or deceleration in the other states. To complete the model, $G = \sigma_\epsilon^2 + \sigma_{stress}^2 I(s_i = 4)$ while $Q = \sigma_{acc}^2$ in states 2 or 3 and 0 otherwise. To make this model easier to compute,

we transform by examining the log of the transition equation and exponentiating the hidden continuous state in the measurement equation. Likelihood evaluation is then performed with the extended Kalman filter (EKF). The EKF is essentially the Kalman filter applied to the first-order Taylor series expansion of any non-linear components around our current predictions of them. For this model, we have

$$\begin{aligned} \log(x_1) &\sim N(x_0, P_0), \\ \log(x_{i+1}) &= \log(x_i) + \log(1 - \mu(s_i)) + \log(\eta_i), \quad \log(\eta_i) \sim N(0, Q(s_i)), \\ y_i &= c(s_i) + \exp(\mathcal{X}_i) + \exp(\mathcal{X}_i)x_i + \epsilon_i, \quad \epsilon_i \sim N(0, G(s_i)), \end{aligned}$$

where \mathcal{X}_i is the estimate of $E[x_i | y_1, \dots, y_{i-1}]$.

We estimated this same model on the entire dataset and performed principal component analysis on the resulting parameters (see also [Section 3.3](#) of the manuscript). [Figure 28](#) shows the inferred performance decisions for Richter’s 1976 performance from both the linear and multiplicative models. Both seem to fit the data quite well. There are three slight differences between the inferences. First, in the B section, the multiplicative model uses the acceleration state more than the additive model does. Second, the multiplicative model avoids the stress state, and this behavior is reflected in a higher probability of remaining in the constant tempo state. Third, the periods of slowing down at the ends of phrases are better explained by the multiplicative model.

The percent of variance explained by the first two principal components is 99%. The first factor loads completely on σ_ϵ^2 while the second loads on μ_{stress} . So, while this model can explain individual performances quite well, it is much less able to provide musically meaningful distinctions between performances. While the interpretation for Richter’s performance seems quite reasonable under this model, other performances are much less reasonable.

A.9 Alternative prior distributions

Following the recommendations of an anonymous referee, we reestimated the model under some alternative prior distributions. These distributions are shown in [Table 7](#). Returning to Richter’s recording, we used inverse gamma and uniform distributions for the variance parameters to allow heavier tails. We also looked at uniform distributions on the transition probabilities and a prior which requires the observation variance, σ_ϵ^2 to be smaller.

Apart from the “smaller observation variance” setting, these different specifications do not have a dramatic effect: the fit to the data remains similar both quantitatively (as measured by RMSE and negative loglikelihood, see [Table 8](#)) and qualitatively (as determined by examining the inferred performance in [Figure 30](#)).

The prior modes are important for some parameters to avoid non-identifiability, and occasionally, as described in the manuscript, to enforce more musically meaningful switching behaviors. On the other hand, the prior tail shape is not particularly important here because we’re estimating posterior modes rather than performing a full Bayesian analysis with accompanying credible intervals.

Table 7: Informative prior distributions for the music model

Parameter	Original	Inverse Gamma		
σ_ϵ^2	\sim Gamma(40, 10)	IG(42, 16400)		
μ_{tempo}	\sim Gamma($\frac{\bar{Y}^2}{100}, \frac{100}{\bar{Y}}$)	IG($\frac{\bar{Y}^2}{100} + 2, \bar{Y}(\frac{\bar{Y}^2}{100} + 1)$)		
$-\mu_{\text{acc}}$	\sim Gamma(15, 2/3)	IG(17, 160)		
$-\mu_{\text{stress}}$	\sim Gamma(20, 2)	IG(22, 840)		
σ_{tempo}^2	\sim Gamma(40, 10)	IG(42, 16400)		
σ_{acc}^2	= 1	1		
σ_{stress}^2	= 1	1		
$p_{1,\cdot}$	\sim Dirichlet(85, 5, 2, 8)	Dirichlet(85, 5, 2, 8)		
$p_{2,\cdot}$	\sim Dirichlet(4, 10, 1, 0)	Dirichlet(4, 10, 1, 0)		
$p_{3,\cdot}$	\sim Dirichlet(5, 3, 7, 0)	Dirichlet(5, 3, 7, 0)		
Parameter	Smaller σ_ϵ^2	Uniform Variances	Uniform Probabilities	
σ_ϵ^2	\sim Gamma(20, 10)	1	Gamma(20, 10)	
μ_{tempo}	\sim Gamma($\frac{\bar{Y}^2}{100}, \frac{100}{\bar{Y}}$)	Gamma($\frac{\bar{Y}^2}{100}, \frac{100}{\bar{Y}}$)	Gamma($\frac{\bar{Y}^2}{100}, \frac{100}{\bar{Y}}$)	
$-\mu_{\text{acc}}$	\sim Gamma(15, 2/3)	Gamma(15, 2/3)	Gamma(15, 2/3)	
$-\mu_{\text{stress}}$	\sim Gamma(20, 1)	Gamma(20, 2)	Gamma(20, 2)	
σ_{tempo}^2	\sim Gamma(40, 10)	1	Gamma(40, 10)	
σ_{acc}^2	= 1	1	1	
σ_{stress}^2	= 1	1	1	
$p_{1,\cdot}$	\sim Dirichlet(85, 5, 2, 8)	Dirichlet(85, 5, 2, 8)	1	
$p_{2,\cdot}$	\sim Dirichlet(4, 10, 1, 0)	Dirichlet(4, 10, 1, 0)	1	
$p_{3,\cdot}$	\sim Dirichlet(5, 3, 7, 0)	Dirichlet(5, 3, 7, 0)	1	

Table 8: For each of the different prior distributions, we report the MSE between the estimated performer intentions from the model and the true performance as well as the negative log likelihood.

prior	rmse	negative log likelihood	σ_ϵ
inverse gamma variances	28.57	-5.20	20.66
original	29.31	-5.10	19.24
smaller variances	26.77	-5.10	20.01
uniform probabilities	30.54	-5.06	21.27
uniform variances	31.05	-5.15	23.56

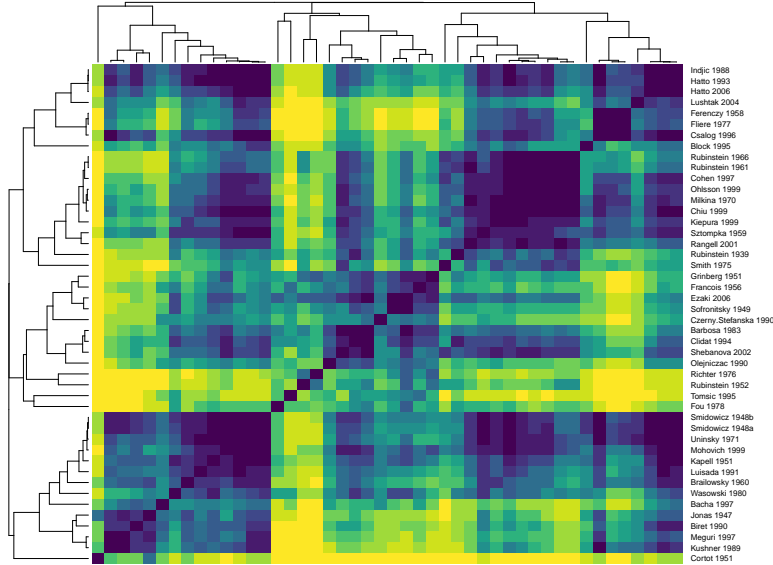


Figure 17: This figure presents a heatmap and hierarchical clustering based only on the note-by-note onset timings for each of the 46 recordings.

Table 9: For each of the different prior distributions, we report the estimated parameter values.

	original	smaller variances	inverse gamma variances	uniform variances	uniform probabilities
σ_{ϵ}^2	426.70	370.37	400.36	452.49	555.29
μ_{tempo}	136.33	167.65	166.55	133.34	135.69
μ_{acc}	-11.84	-23.55	-6.44	-10.02	-7.74
μ_{stress}	-34.82	-16.76	-24.75	-54.16	-50.89
σ_{tempo}^2	439.38	451.58	400.57	406.50	320.17
p_{11}	0.85	0.94	0.91	0.90	0.93
p_{12}	0.05	0.03	0.05	0.02	0.01
p_{22}	0.74	0.46	0.52	0.68	0.85
p_{31}	0.44	0.22	0.30	0.29	0.74
p_{13}	0.02	0.01	0.01	0.01	0.03
p_{21}	0.25	0.47	0.45	0.26	0.08
p_{32}	0.17	0.04	0.20	0.13	0.15

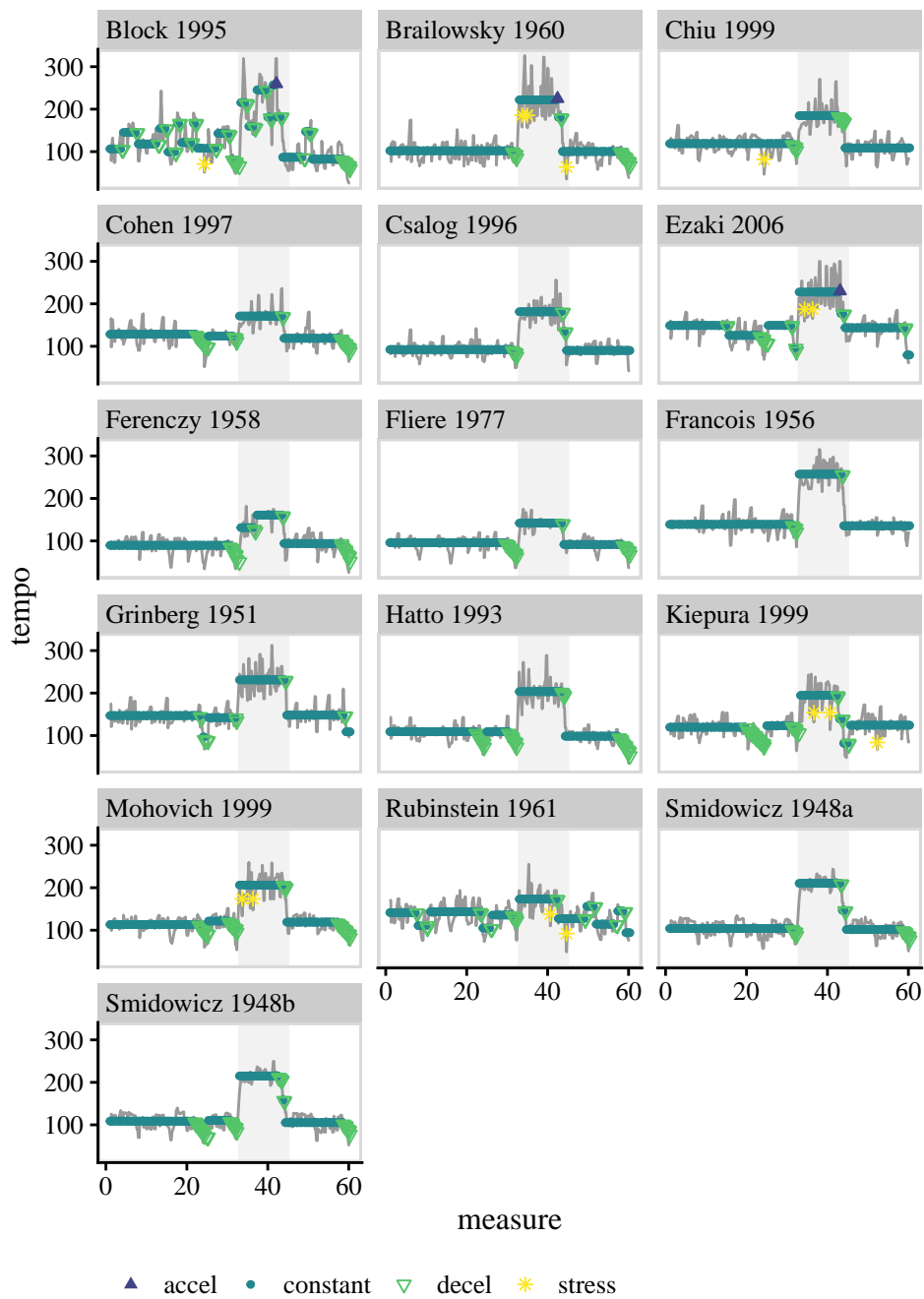


Figure 18: Performances in the first group

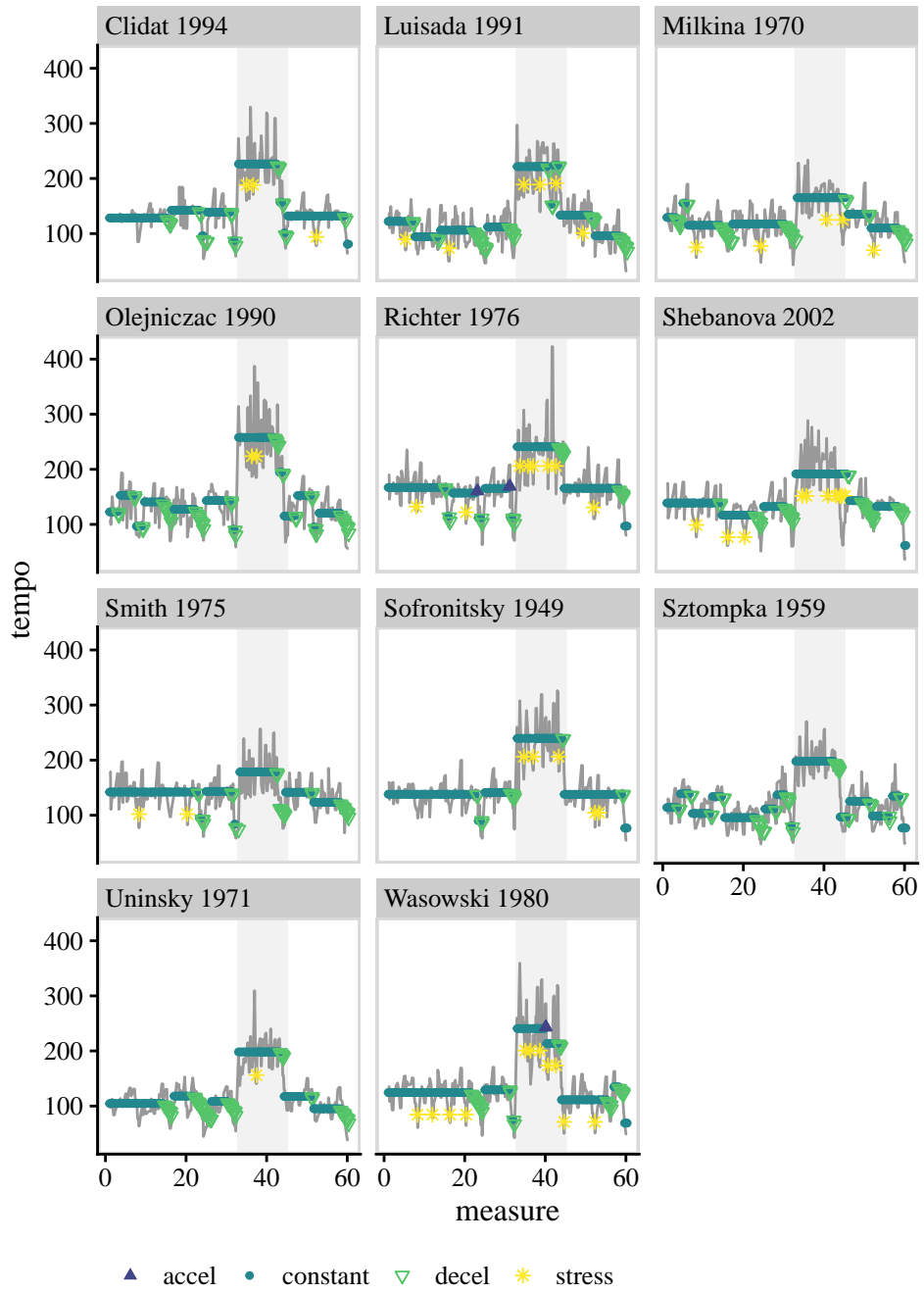


Figure 19: Performances in the fourth group.

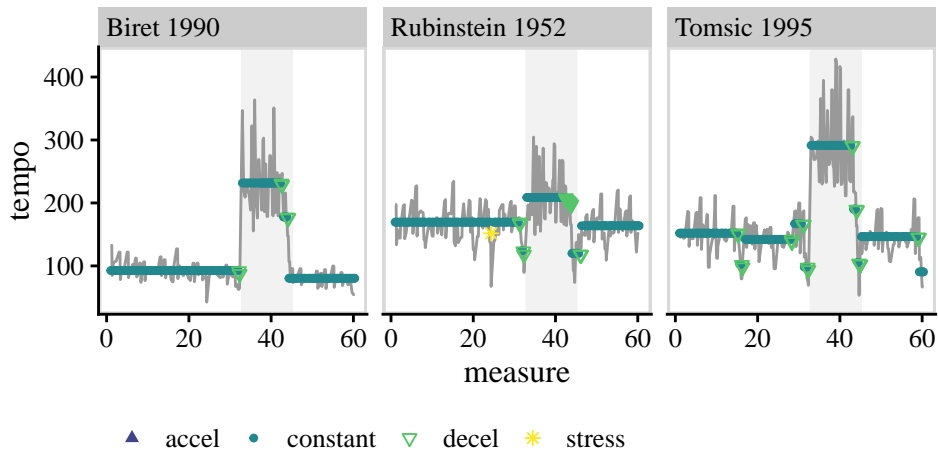


Figure 20: Performances in the sixth group.

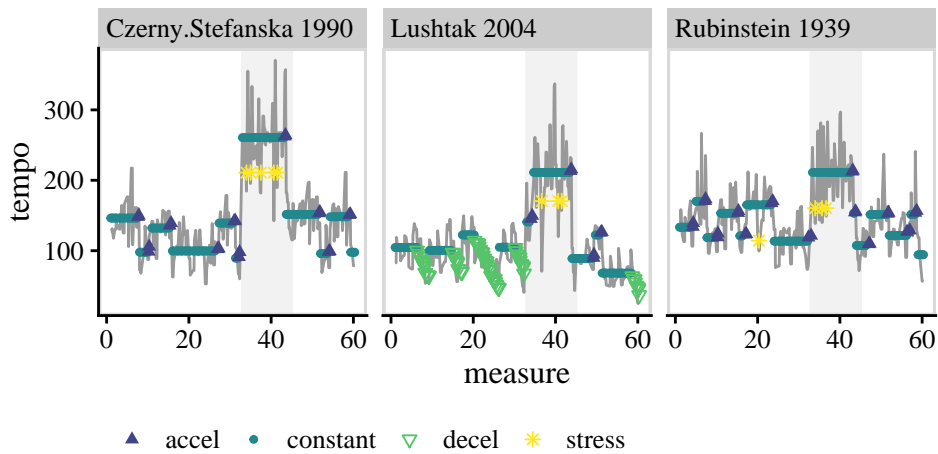


Figure 21: Performances in the second group.

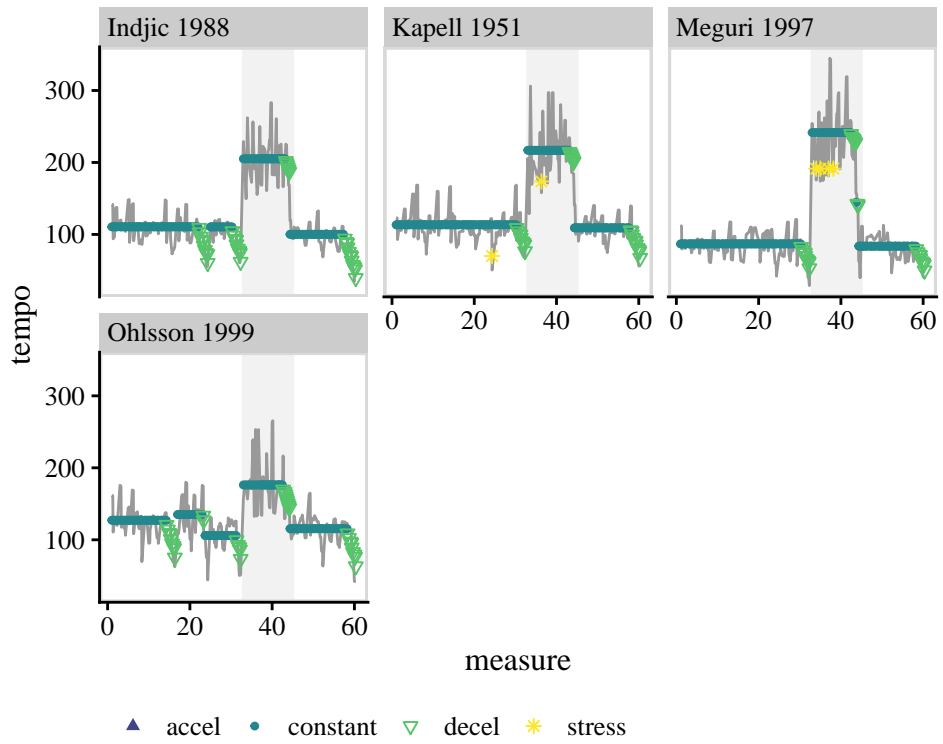


Figure 22: Performances in the third cluster.

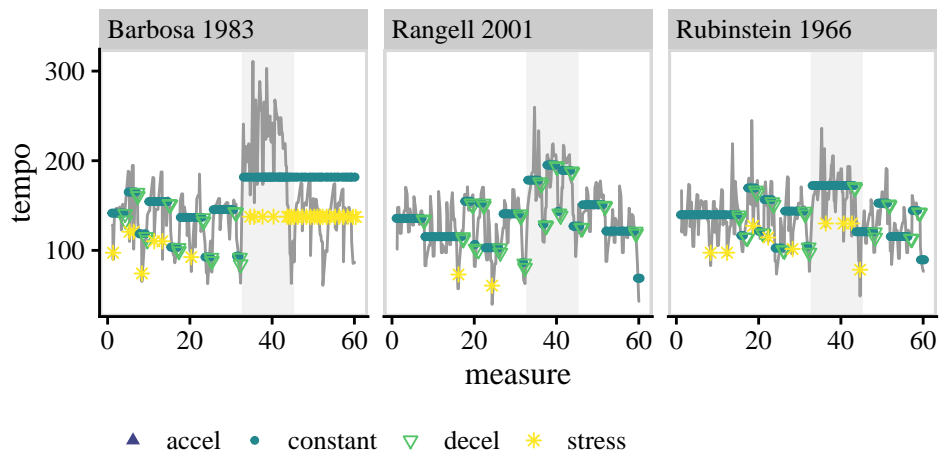


Figure 23: Performances in the fifth group.

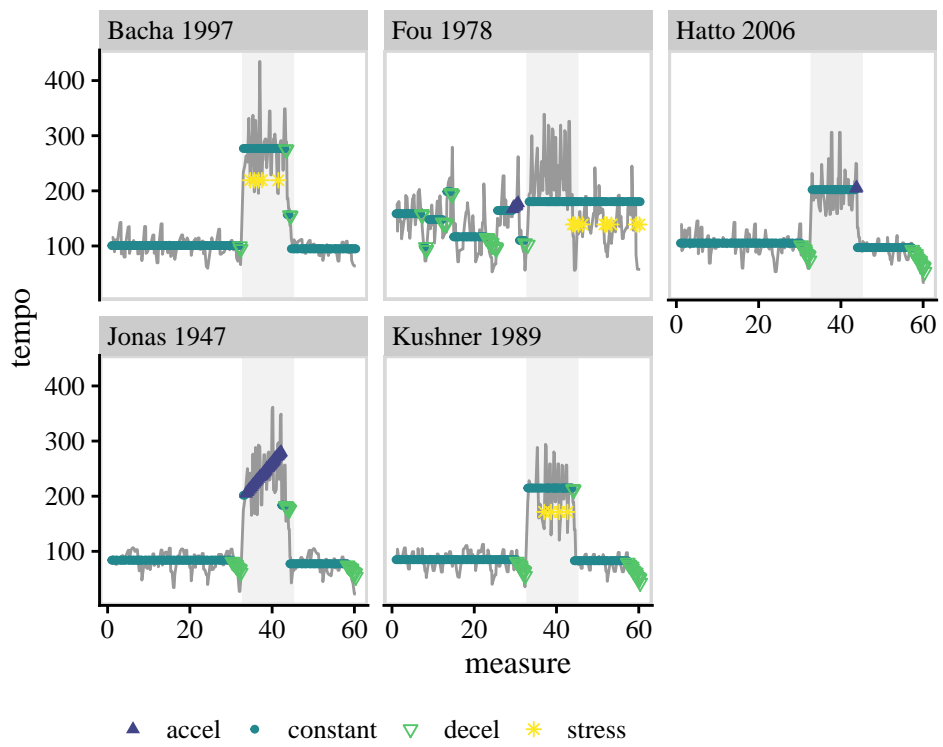


Figure 24: Performances in the seventh group.

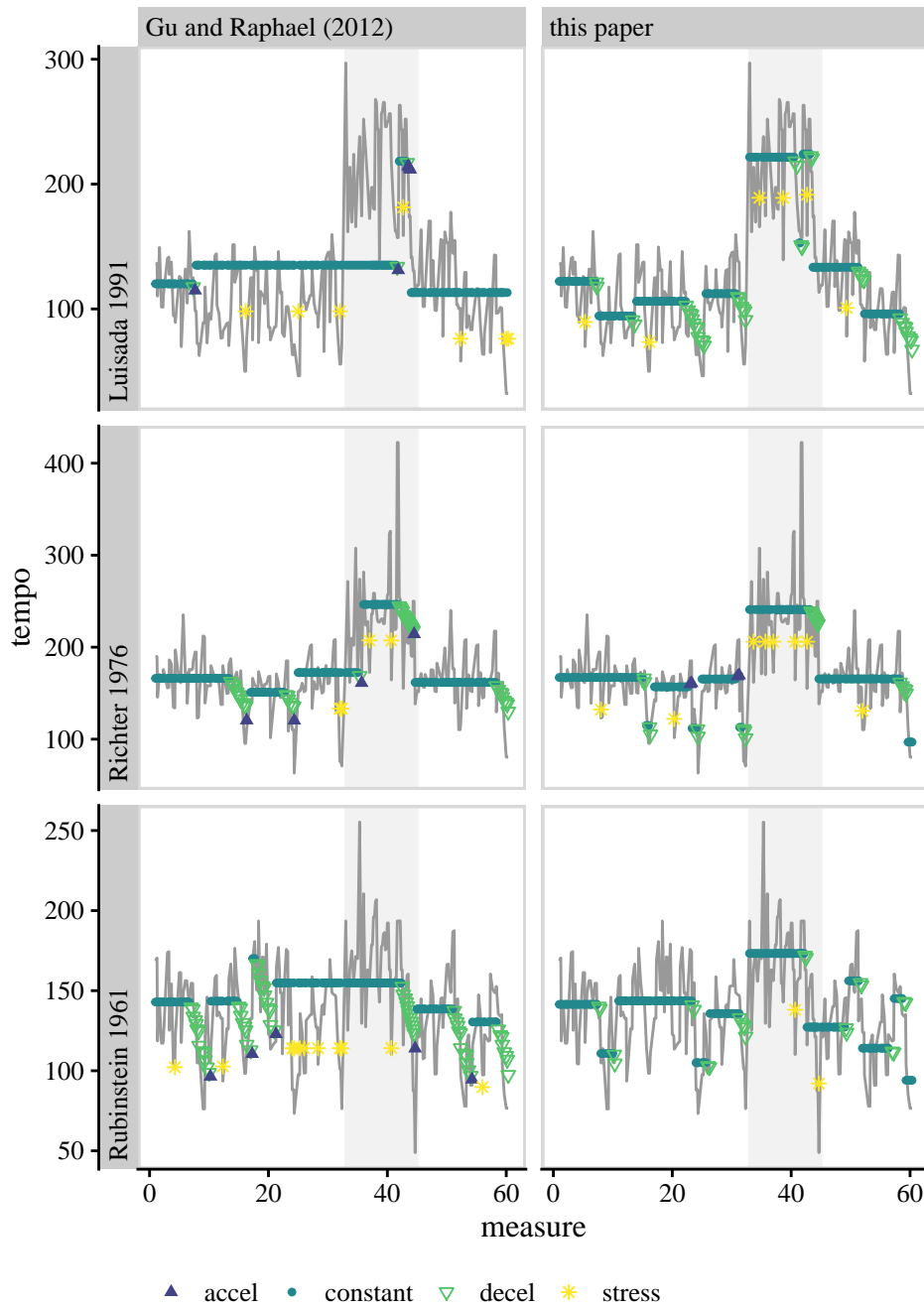


Figure 25: Inferred performance decisions for the tempo model in this paper compared to that examined in previous switching work.

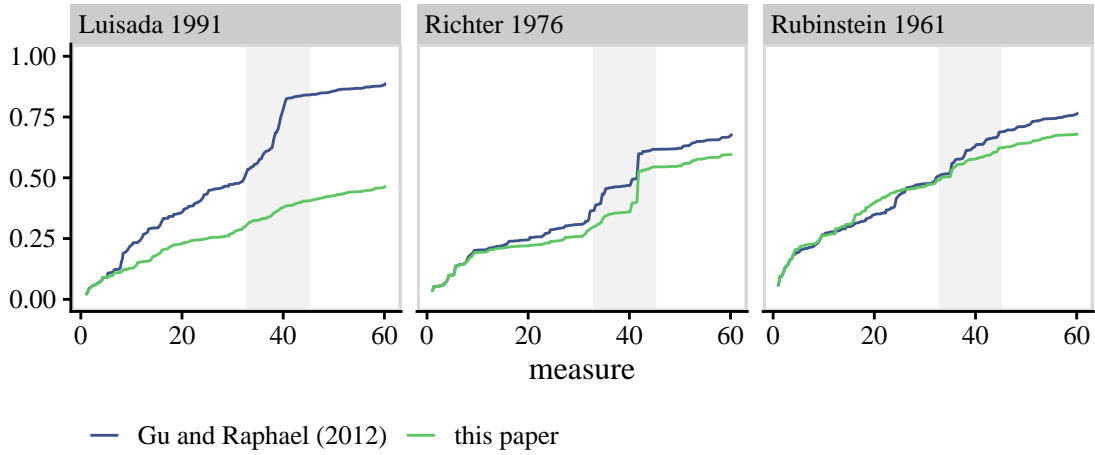


Figure 26: Cumulative RMSE over the recording relative to that of smoothing with the mean (something like $1 - R^2$).

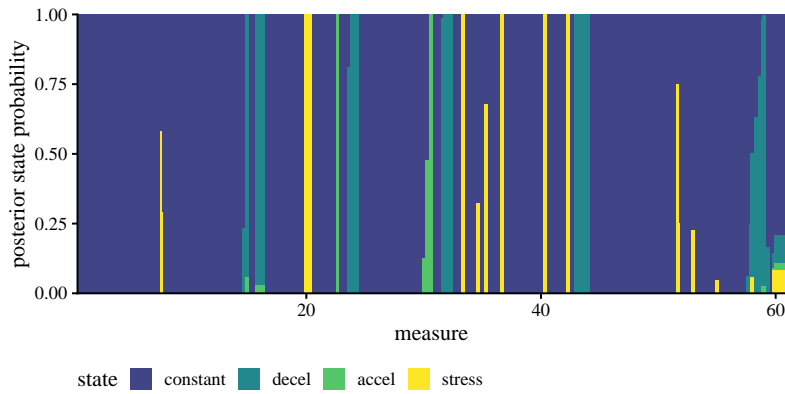


Figure 27: Distribution over potential states for Richter's 1976 recording.

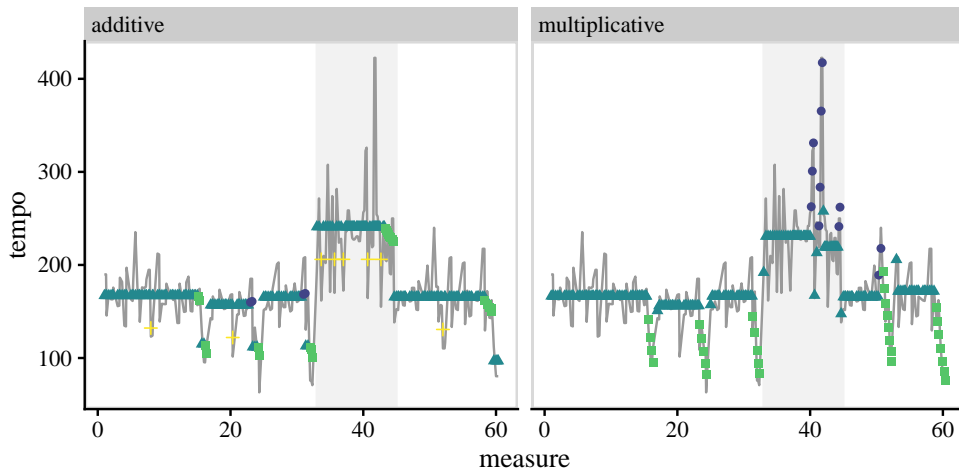


Figure 28: Additive and multiplicative models for Richter's 1976 performance. The multiplicative model fits quite well, but is less likely to visit the stress state.

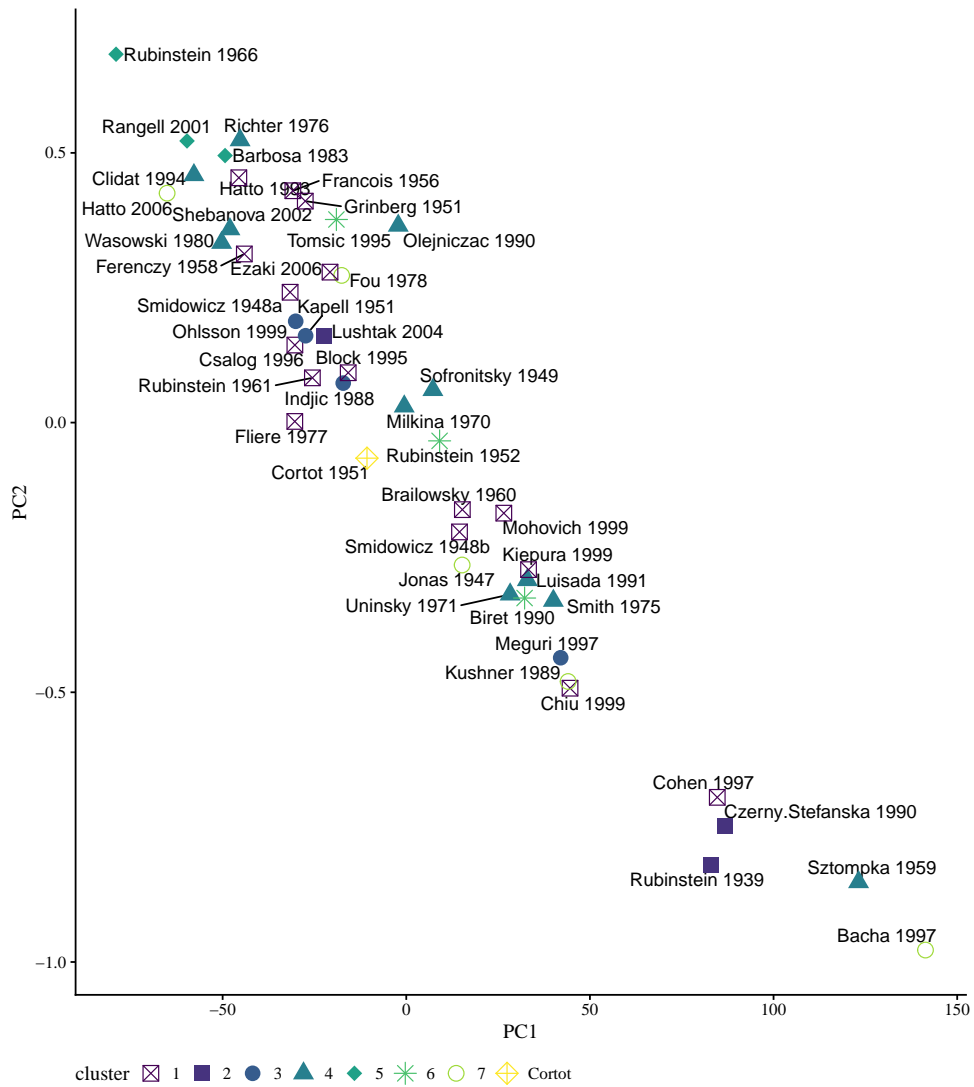


Figure 29: The first two principal components based on parameter estimates from the multiplicative model. The groupings (color and point type) are the same as those from the linear model.

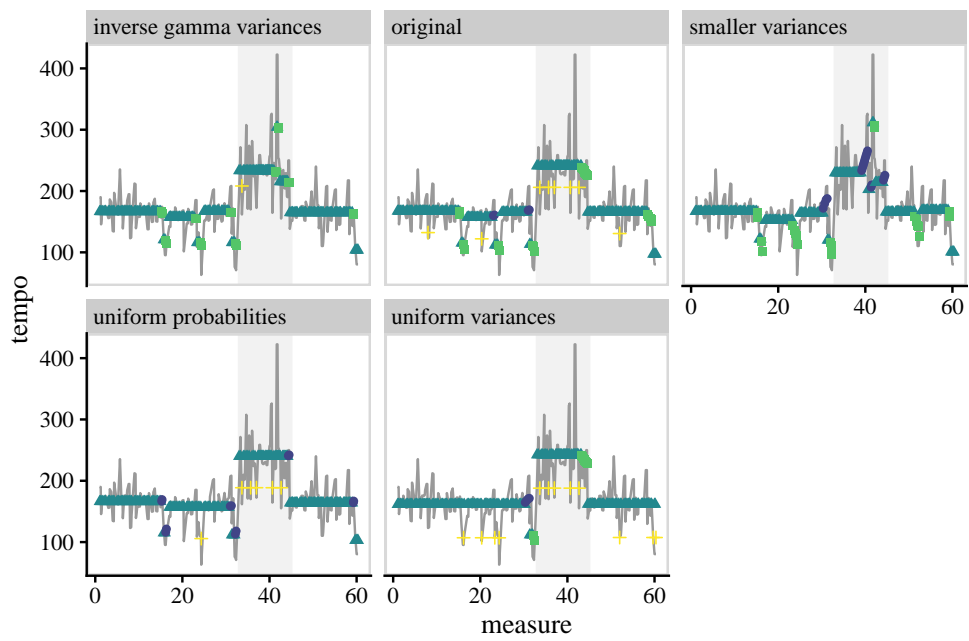


Figure 30: Inferred state sequence for Richter's 1976 recording under alternative prior specifications.